ANL/ESD-14/9 Rev.

Life-cycle Analysis of Bioproducts and Their Conventional Counterparts in GREET™

Energy Systems Division

ANL/ESD-14/9 Rev.

Life-cycle Analysis of Bioproducts and Their Conventional Counterparts in GREET™

by
Jennifer B. Dunn, Felix Adom, Norm Sather, Jeongwoo Han, and Seth Snyder
Energy Systems Division, Argonne National Laboratory

With contributions from Chang He, Jian Gong, Dajun Yue, and Fengqi You
Northwestern University

September 2015

LIFE-CYCLE ANALYSIS OF BIOPRODUCTS AND THEIR CONVENTIONAL COUNTERPARTS IN GREET™

Jennifer B. Dunn, Felix Adom, Norm Sather, Jeongwoo Han, Seth Snyder

Argonne National Laboratory

With contributions from Chang He, Jian Gong, Dajun Yue, and Fengqi You

Northwestern University

CONTENTS

FIGURES

TABLES

ACKNOWLEDGMENTS

This work was supported by the Bioenergy Technology Office (BETO) of the Office of Energy Efficiency and Renewable Energy of the United States Department of Energy, under contract DE-AC02-06CH11357. We are grateful to Travis Tempel, Kristen Johnson, Alicia Lindauer, and Zia Haq of BETO for their support and guidance.

1 INTRODUCTION

1.1 BACKGROUND

Technology to produce biofuels from lignocellulosic feedstocks continues to develop. Recently, INEOS Bio announced that its Indian River BioEnergy Center was the first cellulosic ethanol plant operating at commercial scale in the United States (INEOS Bio 2013). It converts municipal solid waste to ethanol. Additional facilities such as the POET facility near Emmetsburg, Iowa, and the Abengoa facility in Hugoton, Kansas, will produce cellulosic ethanol at commercial scales in the near future (Karlen and Johnson 2014). With these successes in the cellulosic ethanol field, focus is shifting to tapping cellulosic feedstocks to produce drop-in hydrocarbon fuels. These fuels could be directly fungible with existing hydrocarbon fuels and could be transported using existing infrastructure (e.g., pipelines).

Development of technologies to convert cellulosic feedstocks to renewable hydrocarbon fuels is an active area of research (Davis et al. 2013). Economic challenges persist, however, for several reasons. For example, biochemical routes to these fuels may exhibit low yields and consume large amounts of expensive enzymes and other process inputs. Thermochemical routes rely on catalysts used in the upgrading step that are still under development. One perspective on improving the process economics of producing hydrocarbon fuels directly from lignocellulosic feedstocks is to produce bioproducts alongside fuels as value-added biorefinery outputs. Another motivation to produce bioproducts is that their production may be less energy- and emissions-intensive than that of their conventional, fossil-derived counterparts. These potential benefits are important to assess on a life-cycle basis to avoid burden shifting among different life-cycle stages such as feedstock production and conversion. Key metrics to consider when assessing the life-cycle energy and environmental performance of bioproducts are the amount of fossil fuels consumed in their production and the amount of greenhouse gas (GHG) emissions that are produced.

Several researchers have examined the question of the relative energy and environmental performance of bioproducts as compared to their conventional counterparts. For example, Hermann et al. (2007) developed estimates of the life-cycle energy consumption and greenhouse gas (GHG) emissions of 9 bioproducts produced from sugars sourced from corn, sugarcane, or corn stover. The bioproducts were acetic acid, acrylic acid, adipic acid, butanol, caprolactam, ethyl lactate, lysine, ethylene, and succinic acid. Their estimates of the energy and GHG intensities of these compounds were based on process simulations using simplified unit operations calculations that were interchangeable among the processes to produce the compounds in their study. Additionally, Lammens et al. (2011) assessed the life-cycle impacts of producing four compounds from sugar beet vinasse-derived glutamic acid, an amino acid from a low-value byproduct. The compounds were *N*-methylpyrrolidone, *N*-vinylpyrrolidone, acrylonitrile, and succinonitrile. These authors used a consequential rather than a process-based approach to life-cycle analysis (LCA). They concluded that the pyrrolidone compounds offered better performance than their petroleum counterparts, but the same could not be said of the other two compounds included in the study. Finally, Cok et al. (2014) undertook an LCA of succinic acid produced from corn-derived dextrose by three different technologies. They found that

succinic acid produced by fermentation followed by crystallization has a lower life-cycle GHG intensity than fossil-derived maleic, adipic, and succinic acids.

1.2 STUDY DESCRIPTION

To further expand upon the literature in this field and to develop a platform for bioproduct LCA, we developed LCA results for ten bioproducts produced either from algal glycerol or from corn stover-derived sugars. We used Argonne National Laboratory's Greenhouse gases, Regulated Emissions, and Energy use in Transportation (GREET™) model as the platform for this study. The data and calculations reported herein are available to GREET users in a bioproducts module included in the fall 2015 GREET release. This report documents our approach to this analysis and the results. In Chapter 2, we review the process we underwent to select the bioproducts for analysis based on market and technology readiness criteria. In Chapter 3, we review key parameters for production of the two feedstocks we considered: corn stover and algae. Given the lack of publicly available information about the production of bioproducts, which is caused in large part by the emerging nature of the industry, we developed Aspen Plus® simulations of the processes that could be used to produce each bioproduct. From these simulations, we extracted the energy and material flows of these processes, which were important inputs to the GREET bioproducts module. Chapter 4 provides the details of these Aspen Plus simulations. It is important to compare the LCA results for bioproducts to those for their petroleum counterparts. We therefore also developed material and energy flow data for conventional products based mostly on the literature. These data are described in Chapter 5 and are also included in the GREET bioproducts module. In Chapter 6, we present results from this analysis and examine areas for refinement and future research.

It is important to note that the results presented in this report are estimates with relatively high associated uncertainty. The results are characterized this way because the technologies that are used to produce bioproducts are emerging and information about the materials and energy consumed in these processes is limited. Secondly, even though the production of conventional products is mature, publicly available information about material and energy flows for these products is often difficult to find. Nonetheless, this analysis and the GREET bioproducts module provide a means of investigating the relative performance of bioproducts compared to each other and to their conventional, fossil-derived counterparts. Furthermore, this analysis serves to identify the key factors that drive bioproduct LCA results. The GREET module that is a key product of this effort can be used to develop LCA results for additional bioproducts beyond those we considered in this analysis.

2 SELECTION OF BIOPRODUCTS

In this chapter, we review past analyses of commercially significant bioproducts and describe the methodology we used to select the bioproducts that are the focus of this analysis.

2.1 PLATFORM CHEMICALS

In the oil and gas industry, the initial processing of petroleum resources into end-use industrial and consumer products generally takes place in large refineries in which the feedstocks are converted into a small number of chemical intermediates, or platform chemicals. These building-block intermediates are subsequently transported and converted to various end-use products in special-purpose manufacturing plants. Similarly, it is expected that the initial processing of biomass feedstocks will be carried out in large biorefineries that convert the feedstocks into platform chemicals prior to conversion to end-use bioproducts elsewhere. Thus, in order to determine the fossil energy and greenhouse gas (GHG) implications of bioproduct manufacturing, it is necessary to examine both the processes for feedstock conversion to platform chemicals and those for the conversion of these platform chemicals to bioproducts.

In 2004, the U.S. Department of Energy (DOE) produced a report that evaluated a number of candidate platform chemicals that could be produced in biorefineries and prioritized them on the basis of their potential for development into market competitive products (Werpy and Petersen 2004). In a follow-up study in 2010, DOE revisited the 2004 list, taking into account technology advancements and market shifts since the 2004 report was issued (Bozell and Petersen 2010). Table 1 lists the high-potential biorefinery platform chemicals that resulted from these investigations. Those that appear on both lists are highlighted in bold. These two landmark studies provide the basis for the work reported here.

2.2 BIOPRODUCTS

In recent years, there has been growing industrial interest in developing a bioproduct industry, and there is now sufficient publically available information to perform analyses of bioproduct manufacturing processes for a number of them. For example, ethanol, a large-volume fuel product made from corn, is now being developed as a platform chemical for converting cellulosic feedstocks to chemicals. Specifically, ethanol could be dehydrated to produce ethylene, which could in turn be converted to polyethylene. Dow and Braskem both use ethanol in this way. Succinic acid is another very promising (multi-billion pound market) platform chemical that is common to both the 2004 and 2010 lists. It can be converted to a number of end products, including polyesters, phthalic anhydride, and 1,4-butanediol.

An extensive search was conducted of the relevant trade magazines, corporate press releases, patents, and journal publications covering the years since the 2010 report was published to ascertain the current level of industry interest in and commitment to the development of manufacturing processes for bio-based platform chemicals and bioproducts. Of the 20 different

TABLE 1 High-Potential Biorefinery Platform Chemicals

Werpy and Petersen (2004)	Bozell and Petersen (2010)
Aspartic acid	Biohydrocarbons
Fumaric acid	Ethanol
2,5-furandicarboxylic acid	**2,5-furandicarboxylic acid**
Glucaric acid	Furfural
Glutamic acid	**Glycerol**
Glycerol	Hydroxymethylfurfural
3-hydroxypropionic acid	**3-hydroxypropionic acid**
3-hydroxybutyrolactone	Isoprene
Itaconic acid	Lactic acid
Levulinic acid	**Levulinic acid**
Malic acid	**Sorbitol**
Sorbitol	**Succinic acid**
Succinic acid	**Xylitol**
Xylitol	

high-potential platform chemicals on the 2004 and 2010 lists, significant recent industrial interest is evident for nine of them. These are listed in Table 2, which summarizes the conversion processes under development for producing platform chemicals from algal feedstocks and/or corn stover and the bioproducts expected to be manufactured from these platform chemicals. In addition to these nine, sugars are included, which are not on either the 2004 or 2010 list. Sugars are generating substantial industrial interest as potential bio-based platform chemicals.

2.3 SELECTION OF BIOPRODUCTS FOR ANALYSIS

From the various bioproducts listed in Table 2 that can be obtained from the twelve selected platform chemicals, a subset was chosen for analysis of the fossil energy and GHG implications for comparison with their production from fossil feedstocks. To do the down-selection, a meaningful set of criteria for prioritizing the different platform chemical-to-bioproduct processes is required. Considerable guidance for developing these criteria was gleaned from the 2004 and 2010 DOE reports and from discussions with staff at DOE and the National Renewable Energy Laboratory (NREL). To select the bioproducts for inclusion in this analysis, we adopted a qualitative, market-based set of selection criteria defined below:

- Market readiness, as measured by the number of companies currently active in the development of a manufacturing process for the platform chemical.

- Market flexibility, as measured by the number of end-use bioproducts that can be obtained from the platform chemical by processes currently under development.

TABLE 2 Conversion Processes for Bio-Based Platform Chemicals and Bioproducts

Platform chemical	Biomass conversion to platform chemical	Bioproducts	Platform chemical conversion to bioproduct	References
Aspartic acid	Acid hydrolysis of corn stover to glucose followed by microbial fermentation of the glucose	Polyaspartic acid	Polymerization of sodium salt of aspartic acid	Sims 2011, NanoChem Solutions 2013, ChemSystems 1998, Roweton et al. 1997
Ethanol[a]	Acid hydrolysis of corn stover to C_5-C_6 sugars followed by yeast fermentation of the sugars	Ethylene	Dehydration over an acid catalyst at 200–500°C	Westervelt 2013, Fan et al. 2013
		Polyethylene[a]	Ethylene polymerization over $TiCl_3$ or chromium oxide	Gardett 2012, Zhang and Yu 2013, Moser 2013
2,5-Furandicarboxylic acid (FDCA)	Acid hydrolysis of corn stover to C_5-C_6 sugars, catalytic dehydration of the sugars, then catalytic oxidation	Polyethylene furandicarboxylate	Polymerization of ethylene furanoate formed by esterification of FDCA with ethylene glycol	Avantium 2013, Eerhart et al. 2012
Glucaric acid	Acid hydrolysis of corn stover to glucose followed by air or nitric acid oxidation of the glucose	Poly(glucaric acid esters)	Polymerization of esters formed from glucaric acid	Pavone 2012
		Adipic acid	Catalytic hydrogenation	Boussie 2013
Glycerol[a]	Co-product of biodiesel production from algal feedstocks	**Propylene glycol**[a]	Catalytic hydrogenolysis	SRS Engineering Corp. 2013, Xiao et al. 2013
		1-Butanol	Microbial fermentation	Li and Liu 2013, De Greyt et al. 2011, Chen et al. 2014
		1,3-Propanediol (PDO) [a]	Microbial fermentation	Bournay et al. 2005, Posada et al. 2011, Yang et al. 2012
		Epichlorohydrin	Hydrochlorination followed by base addition	Wang et al. 2001, SOLVAY 2010, Bell et al. 2008

TABLE 2 (Cont.)

Platform chemical	Biomass conversion to platform chemical	Bioproducts	Platform chemical conversion to bioproduct	References
3-Hydroxypropionic acid (3-HP) [a]	1) Acid hydrolysis of corn stover to sugars followed by microbial fermentation of the sugars OR 2) Microbial fermentation of glycerol	**Acrylic acid**[a]	Microbial or catalytic dehydration	BASF 2012, Markets and Markets 2013,
		1,3-Propanediol (PDO)[a]	Hydrogenation over Ni or Ni oxide catalyst	Metabolix 2013, Nexant 2013
		Poly(3-HP)	Catalytic conversion to macrocyclic ester followed by catalytic ring-opening polymerization	Andreeßen and Steinbüchel 2010, Zhang et al. 2004, Raj et al. 2008
Isoprene	Acid hydrolysis of corn stover to C_5-C_6 sugars followed by microbial fermentation of the sugars	Polyisoprene rubber	Catalytic polymerization	IHS Chemical 2011, Morgan 2011
Levulinic acid	Acid hydrolysis of corn stover to glucose followed by acid-based or thermolytic dehydration of the glucose	Plasticizers (various)	Polymerization of esters formed from levulinic acid and various alcohols	Segetis 2013, Business Wire 2012, Bozell et al. 2000, Girisuta 2006, Wang et al. 2013b, Chang et al. 2006

TABLE 2 (Cont.)

Platform chemical	Biomass conversion to platform chemical	Bioproducts	Platform chemical conversion to bioproduct	References
Solubilized lignin	Base-catalyzed depolymerization of corn stover followed by acidification and enzymatic hydrolysis	Benzene, toluene, xylene (BTX), and BTX derivatives	Catalytic upgrading of solubilized lignin	Davis et al. 2013
		Phenols and phenolic resins	Catalytic upgrading of solubilized lignin	Holladay et al. 2007
		Adipic acid	Catalytic upgrading of solubilized lignin	Van Duuren et al. 2011
		1,4-Butanediol (BDO)	Catalytic upgrading of solubilized lignin	
		1,3-Butadiene	Catalytic upgrading of solubilized lignin	
		Cyclohexane	Catalytic upgrading of solubilized lignin	VCI 2012
		Carbon fibers	Catalytic upgrading of solubilized lignin	
Succinic acid[a]	1) Acid hydrolysis of corn stover to C_5-C_6 sugars followed by microbial fermentation of the sugars OR 2) Microbial fermentation of co-product glycerol from biodiesel production from algal feedstocks	Poly(butylene succinate)	Condensation polymerization with 1,4-butanediol	Bastidon 2012, Nexant 2012, Pavone 2012
		Adipic acid substitute[a]		BioAmber 2012, Minh et al. 2010, Saleh 2011
		Phthalic anhydride		Dutia 2008
		1,4-Butanediol (BDO)[a]	Aqueous-phase hydrogenation over Re/Ru and Re/Pt	

TABLE 2 (Cont.)

Platform chemical	Biomass conversion to platform chemical	Bioproducts	Platform chemical conversion to bioproduct	References
Sugars[a]	Acid hydrolysis of corn stover followed by supercritical water hydrolysis and enzymatic activation/extraction	**Clean sugars**[a]	Selective crystallization	Sims 2012, Baker 2013, Sweetwater Energy 2013
		Isobutanol[a]	Microbial fermentation	PRWeb 2009, Reisch 2011, Lane 2012, Gevo 2011, Javers 2013, Rivers 2013, DOE EERE 2012, Waite 2012, BlueFire Renewables
L-lactic acid[a,b]	Acid hydrolysis of corn stover to sugars followed by microbial fermentation.	**Ethyl lactate**[a,b]	Reversible esterification	Delgado et al. 2010, Adams and Seider, 2008, Ghaffar et al. 2014, Dusselier et al. 2013.

[a] The platform chemicals and bioproducts included in this analysis are listed in green text were initially included in 2014 GREET release.

[a,b] The platform chemicals and bioproducts included in this analysis listed in green text are updates for 2015 GREET release.

- Market potential, as measured by the current sales and projected sales growth rate for the bioproducts obtained from the platform chemicals

The most recently available information about these market factors for the platform chemicals and bioproducts listed in Table 2 is summarized in Table 3. Products in green font were included in this analysis. References for the information in Table 3 are included in Table 2.

Clearly, using the information in Table 3 to select platform chemical-to-bioproduct processes for analysis requires considerable judgment based on industrial experience. To augment our own experience, we consulted several knowledgeable professionals and, in particular, Gene Petersen of NREL, a co-author of both the 2004 and 2010 DOE reports.

Of the 12 platform chemicals included in Table 2 and Table 3, six are currently being developed as biorefinery platform chemicals by four or more companies. All of these six can be used as feedstocks for multiple bioproducts except for isoprene, which is limited to polyisoprene as an end-use product and hence cannot really be regarded as a platform chemical at this time. These considerations led us to select the remaining six—ethanol, glycerol, 3-hydroxypropionic acid, succinic acid, l-lactic acid, and cellulosic sugars—as the platform chemicals included in this investigation.

Next, the bioproducts obtained from these platform chemicals were selected. In general, these were chosen based on the current market and projected growth rate for the bioproducts. Some, such as poly(3-hydroxypropionic acid) and poly(butylene succinate), have small current markets, while others, for example, phthalic anhydride and cyclohexane, have comparatively small expected growth rates. The choice of succinic acid as a platform chemical is based not only on the bioproducts that can be made from it, but also for its potential as a drop-in substitute for many other dibasic acids (e.g., adipic, malic, and fumaric acids and phthalic anhydride) in a wide variety of applications (De Guzman 2013). The result of this selection process is that six platform chemicals and nine bioproducts were chosen for inclusion in the analysis reported here (1,3-propanediol appears twice, as a bioproduct obtained from both glycerol and 3-hydroxypropionic acid.). The selected platform chemicals and their associated bioproducts are highlighted in green in both Table 2 and Table 3.

The last step in the selection process is to identify the pathways, or conversion processes, that link the platform chemicals with their respective bioproducts. In some cases, multiple conversion routes were possible. For example, succinic acid and 3-hydroxypropionic acid can both be made from either glycerol or cellulosic sugars by known conversion processes. Whenever there were conversion pathway alternatives, we selected the one having the most complete publically available conversion process information (equipment, operating conditions, chemical reactions, conversion, and selectivities). Figure 1 shows the chemical processing pathways that link the production of the selected platform chemicals from either algal feedstocks or corn stover and the manufacture of the selected bioproducts from them.

TABLE 3 Market Factors for Platform Chemicals and Bioproducts

Platform chemical[a]	Market readiness as measured by the number of active companies	Market flexibility as measured by the major end-use bioproducts	Market potential as measured by sales and projected growth rate
Aspartic acid	Flexible Solutions, NanoChem Solutions	Polyaspartic acid	Small current sales but growth potential is high
Ethanol[a]	Dow, Braskem, Solvay, Royal DSM/ POET	Ethylene	129 Mmt (U.S. 2012)/4% growth rate
		Polyethylene[a]	60% of total ethylene demand/5%
2,5-Furandicarboxylic acid (FDCA)	Avantium, Wageningen UR	Polyethylene furandicarboxylate	No current market, potential polyethylene terephthalate replacement
Glucaric acid	Rivertop Renewables, Rennovia	Poly(glucaric acid esters)	No current market, new product
Glycerol[a]	ADM, Cargill, Solvay, Dow, Senergy, Virent, Cobalt Technologies	**Propylene glycol[a]**	1.7 Mmt (global 2008)
		1-Butanol	$5B (global 2010)/11%
		1,3-Propanediol (PDO)[a]	$0.16B (global 2012)/20%
		Epichlorohydrin	1.5 Mmt (global 2012)/4.8%
3-Hydroxypropionic acid (3-HP)[a]	Cargill/Novozymes/BASF, OPXBio/Dow Chemical, Metabolix, Myriant, Gemomatica, Arkema	**Acrylic acid[a]**	4.5 Mmt (global 2011)/4%
		1,3-Propanediol (PDO)[a]	$0.16B (global 2012)/20%
		Poly(3-HP)	New product with negligible current market
Isoprene	Bridgestone/Aginomoto, Goodyear/DuPont Industrial Sciences, Michelin/Amyris, Glycos Biotechnologies, Aemetis	Polyisoprene rubber	0.7 Mmt (2011), 5% of the total isoprenic elastomer (rubber) market
Levulinic acid	Incitor, Segetis/Georgia Gulf, Avantium	Plasticizers (various)	No information available

TABLE 3 (Cont.)

Platform chemical	Market readiness as measured by the number of active companies	Market flexibility as measured by the major end-use bioproducts	Market potential as measured by sales and projected growth rate
Solubilized lignin	Wageningen UR, Lignol	BTX and BTX derivatives	85 Mmt (2010)
		Phenols and phenolic resins	No information available
		Adipic acid	3 Mmt (global 2010)
		1,4-Butanediol (BDO)	1.72 Mmt (global 2011)/5.5%
		1,3-Butadiene	$22B (global 2011)/8%
		Cyclohexane	5.3 Mmt/3%
		Carbon fibers	0.11 Mmt (global 2012)
Succinic acid[a]	BASF/Purac, Myriant, Reverdia, BioAmber,	Poly(butylene succinate)	0.015 Mmt (global 2010)
	Verdezyne	**Adipic acid substitute**[a]	2.3 Mmt (global 2012)/5%
		Phthalic anhydride	4.2 Mmt (global 2008)/3%
		1,4-Butanediol (BDO)[a]	1.72 Mmt (global 2011)/5.5%
Sugars[a]	Renmatix/BASF, Virdia, Sweetwater Energy, Comet Biorefining, Proterro, ICM, Red Shield, BlueFire Renewables	**Clean sugars**[a]	Undetermined, but has a large upside potential
		Isobutanol[a]	1.1 billion gal (global 2010) for use as a chemical
L-lactic acid[a,b]	NatureWorks LLC, Corbion Purac, PGLA-1,Galactic Anhui BBCA & GALACTIC Lactic Acid Company Limited (B&G), Musashino	**Ethyl lactate**[a,b] Polylactic acid Acrylic acid 2,3 Pentanedione	0.15 Mmt (global 2000)
Ethyl lactate[a,b]	Galactic, Vertec Biosolvents	Industrial solvent (Various)	Undetermined but the IEA suggest 80% of conventional solvents could be replaced by

	ethyl lactate[c]

[a]The platform chemicals and bioproducts included in this analysis are listed in green text were initially included in 2014 GREET release.

[a,b] The platform chemicals and bioproducts included in this analysis listed in green text are updates for 2015 GREET release.

[c]http://www.iea-bioenergy.task42-biorefineries.com/upload_mm/b/a/8/6d099772-d69d-46a3-bbf7-62378e37e1df_Biobased_Chemicals_Report_Total_IEABioenergyTask42.pdf

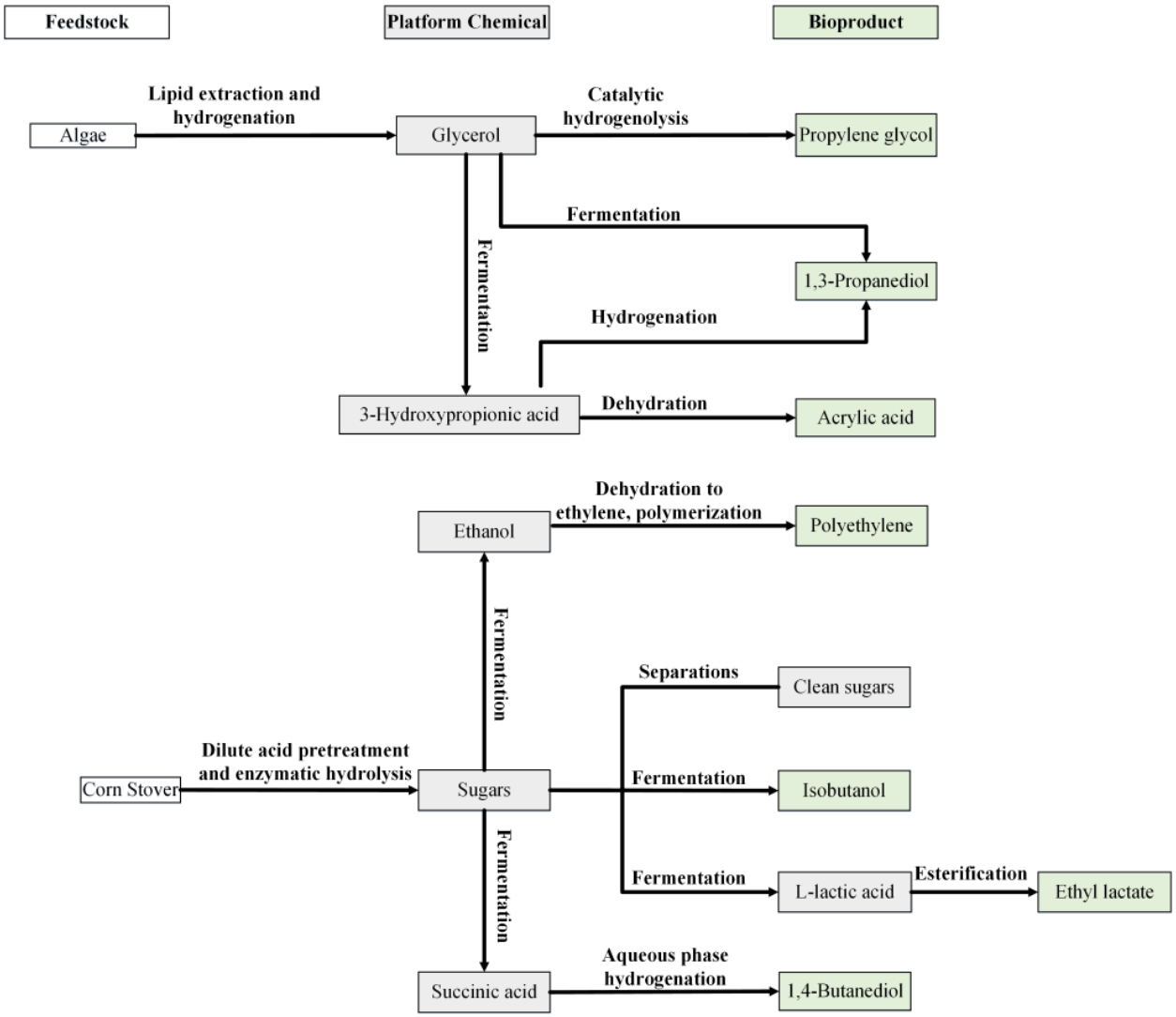

FIGURE 1 Platform Chemicals and Bioproducts Selected for Analysis

In the context of this study (Figure 1), platform chemicals (e.g. 3-hydroxypropionic acid, L-lactic acid) are considered to be bioproducts.

3 FEEDSTOCKS

The life cycle of each of the platform chemicals and bioproducts we consider in this report begins with either the production of algae or the recovery of corn stover as a by-product of corn agriculture. In the following two sections, we summarize how these feedstocks are handled in GREET based on previous and ongoing research.

3.1 CORN STOVER

A separate technical report (Wang et al. 2013c) provides a complete description of the development of corn stover parameters in GREET. To summarize, the underlying assumption regarding the treatment of corn stover in the model is that it is essentially an agricultural waste produced as a by-product of corn agriculture. Currently, we assume that corn stover is collected in a second pass of agricultural equipment after the harvest of corn grain. Single-pass harvest systems are now under development, and GREET treatment of this feedstock may be revised as the technology matures and is implemented. Additionally, the removal of corn stover from corn fields prevents the nutrients in the removed stover from reincorporating into the soil. Currently, we assume that the nutrient content of the removed stover must be replaced with conventional fertilizer on an equal-mass basis. It may emerge that less fertilizer application is needed as the agricultural community gains experience with corn stover removal. Finally, we have assessed land-use change (LUC) associated with the production of corn stover ethanol and found it to be essentially negligible (Dunn et al. 2013). For this reason, we do not incorporate any LUC GHG emissions from the production of bioproducts from corn stover.

3.2 ALGAE

GREET modeling of algae production is based on the results of a harmonization effort to unify the assumptions behind the techno-economic and LCA modeling of algal fuels among Argonne National Laboratory, NREL, and Pacific Northwest National Laboratory (Davis et al. 2012). Algae are produced in a facility having ponds 4,050 ha in area. During algae growth, diammonium phosphate (DAP) and ammonia are provided as nutrients; CO_2 is provided by flue gas delivered by a low-pressure pipeline. Key electricity consumers during algae production include pumping, centrifugation, and homogenization. Lipid extraction produces the algal oil feedstock used for production of bioproducts. Because algae are not a terrestrial feedstock, no LUC is associated with its production.

4 MATERIAL AND ENERGY FLOW DATA FOR BIOPRODUCTS

To estimate the materials and energy consumed in the production of the platform chemicals and bioproducts we selected (Figure 1), we developed process simulations in Aspen Plus. The key parameters used in these simulations (yield, reaction temperature, consumption of materials) were based on trade journal articles, technical reports, and patents and patent applications. It remained necessary to use assumptions and engineering judgment to develop full simulations, given the limited amount of information available in the public domain.

Several overarching issues affect all simulations. First, the selection of an appropriate thermodynamic property model was a critical aspect of process modeling. Two property estimation methods were used in our models. The first was the Peng Robinson property method, which is suitable for non-polar or mildly polar mixtures such as hydrocarbons and light gases (e.g., hydrogen gas). It is particularly suitable for high-temperature and high-pressure processes. The non-random, two-liquid (NRTL) property method, on the other hand, is suitable for non-ideal chemical systems and estimates vapor-liquid phase equilibria with binary interaction coefficients of chemical components. Secondly, we harmonized feedstock production assumptions so that upstream impacts would align for all processes using either corn stover or algae as a feedstock. For processes with an algal feedstock, we assumed technical grade glycerol (98%) was produced from algae via lipid extraction and hydrogenation.

For each process consuming glycerol, the feed rate was 1,000 kg/hr based on expected algae production in the United States (Davis et al. 2013). In the case of processes consuming 3- hydroxypropionic acid as a feedstock, the feed rate was 6,500 kg/hr. Another group of bioproducts use clean sugars as the starting material. Our model of the production of this feedstock from corn stover was based on Humbird et al. (2011) for the biochemical production of ethanol. We used the clean sugars output from the hydrolysis reactor as the input to the clean sugars-based processes we simulated. Humbird et al. (2011) adopted NRTL as the property estimation method and assumed a corn stover supply of 2,205 of dry tons/day. Clean sugars were then produced at 69,400 dry kg/hr, which served as the feed rate for all clean sugars-based processes in our analysis except L-lactic acid. For that compound, we based sugar production capacities on mid-sized commercial plants (Corbion Purac 2015; Ullmann's Encyclopedia of Industrial Chemistry 2015). As a result, an average of 7,400 dry kg/hr clean sugars was assumed as the throughput for the L-lactic process.

In the simulations we developed, we used heat integration, capturing useful rejected heat for utilization in other unit operations. The heuristic we used to identify useful rejected heat was that the difference in temperature between the unit operations rejecting and receiving heat had to exceed 20°C.

The following subsections provide detailed descriptions of each of the process simulations developed for this study and material and energy flow results used as GREET inputs. We assumed process heating demands were met with 80% efficient natural gas-fired boilers; reported energy intensities reflect this assumption.

4.1 GLYCEROL TO PROPYLENE GLYCOL

Figure 2 summarizes the key unit operations modeled in the production of propylene glycol (PG) from technical grade glycerol. The key process steps are preheating of the feed mixture, propylene glycol synthesis via hydrogenation, and distillation of the liquid phase product stream to achieve market purity grade PG (98 wt%).

The glycerol feed is pressurized to 40 bar and subsequently heated from ambient temperature to about 188°C before entering the reactor (R-101). PG synthesis is achieved via hydrogenation using two stoichiometric reactors in series (R-101 and R-102). Reaction conditions for the stoichiometric reactors are based on a patent (Ding et al. 2013). The authors report a low capital cost and attractive technology for the conversion of glycerol to PG. A proprietary catalyst comprising a metal or metal oxide dispersed on an inert support is used for the hydrogenation reaction for PG synthesis. The first reactor (R-101) converts glycerol to an intermediate product (acetol). The second reactor (R-102) subsequently converts the acetol via hydrogenation to PG and other co-products (1-propanol and isopropyl alcohol). Parametric specification of the reactors in Aspen Plus such as stoichiometric reactions, yields, temperature, and pressure are summarized in Table 4 and Table 5.

After the hydrogenation reaction, the R-102 effluent is a mixture of residual glycerol (12wt%), PG (72 wt%), H_2O (10 wt%), H_2 (5 wt%), and other components (1 wt%). This stream is flashed (Flash-101) and the liquid phase effluent from Flash-101 is sent to a holding tank (not shown) prior to distillation, which recovers purified PG. The vapor phase from Flash-101 is cooled (Cooler-101) and sent to Flash-102. After flashing in Flash-102, the vapor phase effluent, mainly H_2 gas, is recovered and pressurized using a compressor (Compr-101). This stream is

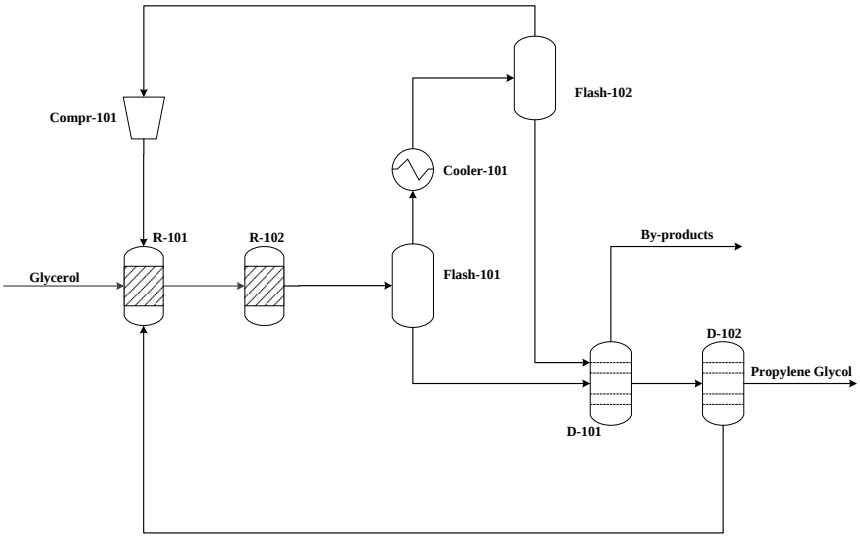

FIGURE 2 Simplified Process Flow Diagram of Glycerol-to-PG Process

TABLE 4 Summary of Assumed Stoichiometric Reactions and Yields for the Glycerol-to-PG Process

	Reaction	Reactant	Percent converted to product (by mass)
1	Glycerol → H_2O + Acetol	Glycero1	75
2	Acetol + H_2 →Propylene glycol	Acetol	95
3	Acetol + H_2 → 1-Propanol + H_2O	Acetol	1.0
4	Acetol + H_2 → Isopropyl alcohol + H_2O	Acetol	0.50

TABLE 5 Summary of Parameters Used in Key Unit Operations

Unit operation	Aspen Plus ID	Modeling parameters
Reactor (R-101)	RSTOIC	Pressure: 38 bar Temperature: 190°C
Reactor (R-102)	RSTOIC	Pressure: 38 bar Temperature: 200°C
Distillation column (D-101)	RadFrac	Condenser pressure: 1.4 bar Condenser temperature: 54°C Stages: 16 Molar reflux ratio: 0.5 Bottoms rate: 36 kmol/hr
Distillation column (D-102)	RadFrac	Condenser pressure: 1 bar Stages: 15 Molar reflux ratio: 0.1 Bottoms rate: 36 kmol/hr
Compressor	Compr	Isentropic Pressure: 41 bar

subsequently recycled to R-101. The liquid phase effluent from Flash-102 is sent to the holding tank and subsequently to the product purification and recovery section of the plant.

Two distillation towers (D-101 and D-102) in succession are used to purify the PG stream. The first distillation column separates the by-products and some water from PG. A second column is required to reach 98 wt% PG. Recovered process water is recycled back to R-101. Specific design assumptions for the major unit operations are summarized in Table 5.

Table 6 summarizes the overall material and energy intensity for this process. For this and all modeled processes, we assumed that 80% efficient natural gas boilers produce steam. For this process, we therefore estimated that approximately 7.2 MMBtu natural gas per ton of PG is

TABLE 6 Mass and Energy Intensity: Glycerol to PG

Energy Inputs	*MMBtu/ton*
Natural gas	7.2
Electricity	0.36
Material Inputs	*ton/ton*
Glycerol	1.4
Hydrogen	3.5×10^{-2}

required to meet the plant heat demand. The distillation columns consume about 95% of the process heat demand; heaters consume the balance. As is the case with most of the processes we modeled, pumps consume a minor amount of electricity.

4.2 GLYCEROL TO 1,3-PROPANEDIOL (1,3-PDO)

Figure 3 summarizes the simplified flow diagram for the glycerol to 1,3-PDO process. Briefly, after feedstock sterilization, 1,3-PDO is produced via fermentation and subsequent recovery and purification of the product stream.

In the model, the fermentation medium consists of KH_2PO_4 and glycerol. This mixture is sterilized at 121°C for 15 minutes and subsequently cooled to the fermentation temperature prior to passing to the fermentation reactor (R-101). *Klebsiella pneumonia* was adopted as the bacterial strain for the fermentation process (Ma et al. 2009), and the fermentation residence time and temperature were taken to be 48 hours and 40°C, respectively (Ma et al. 2009). After fermentation, the product stream is flashed (Flash-101) and subsequently centrifuged to remove fermentation gases and cell mass, respectively. The clarified broth that emerges from the centrifuge is sent to product recovery and purification to concentrate the 1,3-PDO stream to market purity (98 wt%). Table 7 summarizes the reactions and corresponding yields assumed in the fermenter.

The product recovery and purification section begins with aqueous phase liquid-liquid extraction (LLE) of the 1,3-PDO from the clarified fermentation broth that we modeled based on a report by Chung et al. (2012). These authors reported a low-cost extraction process to separate 1,3-PDO from water at an efficiency exceeding 90% using a hydrophilic alcohol/salt mixture (ethanol/K_2HPO_4). In our design, the LLE process is modeled using the component separator unit operation with an extraction efficiency of 95%. We assume that the LLE column consumes a negligible amount of energy. After LLE, the concentrated 1,3-PDO stream is pumped and heated from 30 to 85°C before going to a 16-stage distillation column. The production rate of 1,3-PDO (100 wt%) is 524 kg/hr.

Table 8 summarizes key process parameters, and the overall material and energy intensity of the process is summarized in Table 9. Operation of the distillation column consumes about 95% of the natural gas demand; heaters consume the rest.

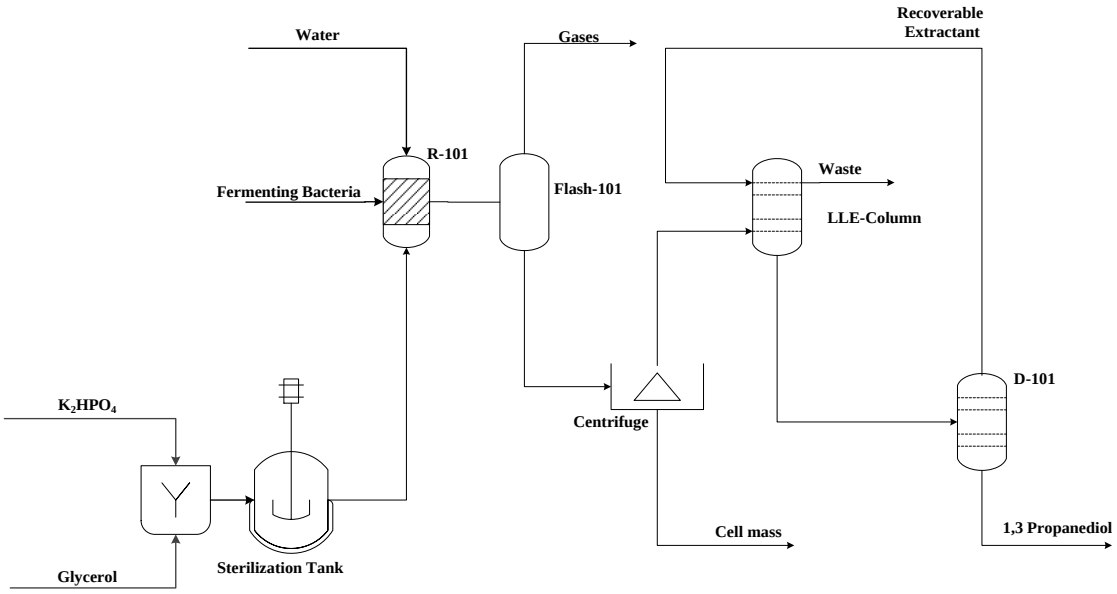

FIGURE 3 Simplified Process Flow Diagram for Glycerol to 1,3-PDO

TABLE 7 Summary of Assumed Stoichiometric Reactions and Yields for Glycerol to 1,3-PDO

	Reaction	Reactant	Percent converted to product (by mass)
1	Glycerol + O_2→ 0.63 1,3-PDO + 0.1 Acetic acid + 0.1 Ethanol + 2.182 H_2O + H_2 + 0.71 CO_2	Glycero1	51
2	Glycerol+ K_2HPO_4 + → 4.97 Cell mass + 8 H_2O	K_2HPO_4	48

TABLE 8 Summary of Key Process Parameters

Unit operation	Aspen Plus ID	Modeling parameters
Reactor (R-101)	RSTOIC	Pressure: 1 bar Temperature: 37°C
Distillation column	Radfrac	Condenser pressure: 1 bar Stages: 16 Molar reflux ratio: 1.0×10^{-4} Bottoms rate ratio: 524 kg/hr

TABLE 9 Mass and Energy Intensity: Glycerol to 1,3-PDO

Energy Inputs	*MMBtu/ton*
Natural gas	13
Electricity	0.10
Material Inputs	*ton/ton*
Glycerol	2.0
Oxygen	0.63
K_2HPO_4	0.63

4.3 GLYCEROL TO 3-HYDROXYPROPIONIC ACID (3-HP)

The overall process design for the conversion of glycerol to 3-HP consists of three key sections: sterilization, fermentation, and product recovery and purification, as Figure 4 illustrates.

The glycerol feedstock is mixed with the fermentation media, which contains mostly disodium phosphate (Na_2HPO_4) solution, a nitrogen source for the fermenting organism. The mixed stream is sterilized at 121°C for 15 minutes and subsequently cooled to the fermentation temperature prior to passing into the fermentation tank (R-101).

Modeling parameters and assumptions for the fermentation process are based on Raj et al. (2008). 3-HP is produced by a recombinant strain of *Escherichia coli* at 37°C over a 48-hr period. Arabinose is added to the fermentation tank as an additional carbon source supplement for the bacteria strain. Table 10 summarizes the assumed stoichiometric reactions and yields used in our model. After the fermentation process, the broth containing about 27 wt% 3-HP is subsequently centrifuged to remove cell mass before product recovery and purification.

Downstream purification of the clarified broth to obtain 3-HP can be achieved by either distillation or electrodeionization (EDI). Both routes were investigated. In the case of distillation, the broth is heated to about 70°C and run through a 20-stage distillation column (D-101). This results in approximately 30 wt% concentration of 3-HP in the product stream. The EDI unit results in a product purity of 30 wt%. The EDI unit was modeled using the component separator unit operation in Aspen Plus. We assumed 95% recovery of 3-HP in the EDI concentrated product effluent stream with approximately 30 wt% concentration. We assumed that the EDI unit consumes approximately 2,930 kWh electricity/ton 3–HP (10 MMBtu/ton) (Lin 2013). It is worth noting that 3-HP market purity varies (30–95%)[1,2,3] depending on the vendor. Table 11 summarizes the key parametric assumptions for the major unit operations for these processes.

[1] http://www.sigmaaldrich.com/catalog/product/aldrich/cds000335?lang=en&region=US
[2] https://us.vwr.com/store/catalog/product.jsp?product_id=4547124
[3] http://www.apolloscientific.co.uk/display_item.php?id=52262

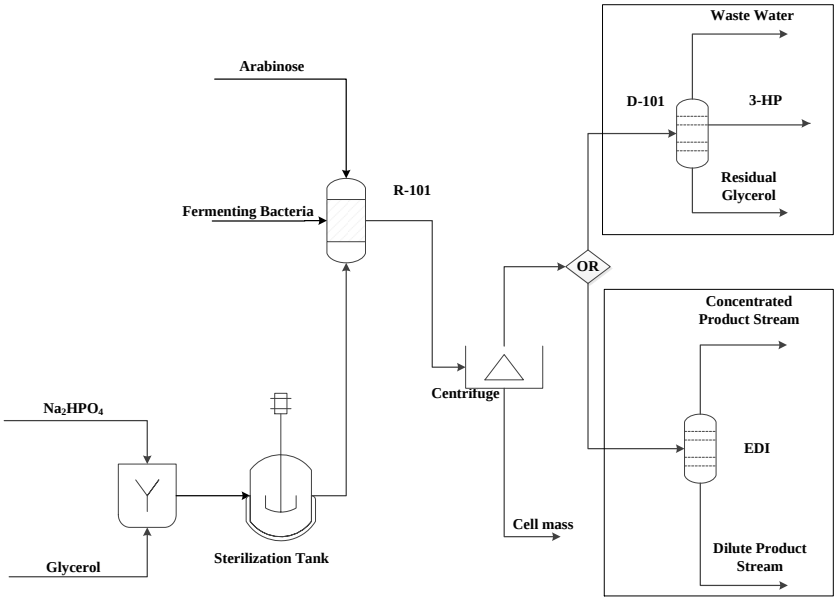

FIGURE 4 Simplified Process Flow Diagram for Glycerol to 3-HP

TABLE 10 Summary of Assumed Stoichiometric Reactions and Yields (Raj et al. 2008)

	Reaction	Reactant	Percent converted to product (by mass)
1	Glycerol → 3-HP + Hydrogen	Glycerol	50
2	Glycerol → Lactic acid + Hydrogen	Glycerol	0.10
3	Glycerol + H_2O → Acetic acid + CO_2+ 3 Hydrogen	Glycerol	0.10
4	Glycerol → Ethanol + CO_2+ Hydrogen	Glycerol	0.10
5	Arabinose + Na_2HPO_4 → 6.01496 Biomass+ 8 H_2O	Arabinose	5.0
6	Glycerol + Na_2HPO_4→ 3.65571 Biomass+ 8 H_2O	Glycerol	5.0

TABLE 11 Summary of Parameters Used in Key Unit Operations

Unit operation	Aspen Plus ID	Modeling parameters
Reactor (R-101)	RSTOIC	Pressure: 1 bar Temperature: 37°C
Distillation column (D-101)	RadFrac	Condenser pressure: 0.1 bar Stages: 20 Molar reflux ratio: 0.1 Distillate to feed ratio: 0.75
EDI	Component Separator	95% separation efficiency of 3-HP

Table 12 summarizes the overall material and energy intensity for the process. The key drivers were natural gas and electricity demand in the distillation column and the EDI unit, respectively.

4.4 3-HYDROXYPROPIONIC ACID TO ACRYLIC ACID

Figure 5 summarizes the acrylic acid production process. The feedstock (3-HP) for this process is assumed to be produced from algal glycerol as Section 4.3 describes. The key process steps in Figure 5 are dehydration and distillation.

This process consumes 69,400 kg/hr of 3-HP (30 wt%) which is mixed with 25 kg/hr of H_3PO_4 acid prior to entering the dehydration reactor (R-101). The formation of acrylic acid proceeds via homogeneous acid-catalyzed thermal dehydration of 3-HP in the liquid phase at a low pressure. Reported yields of acrylic acid are catalyst-dependent and range from 50 to 90%. The assumed yield for this simulation is based on a patent by Craciun et.al (2009). The reaction is exothermic; cooling is required to maintain the reaction temperature at 80°C. Table 13 reports the dehydration reaction stoichiometry and yield. Additional parametric assumptions for reactor design are reported in Table 14.

The effluent from R-101 is purified in two distillation columns. The first 10-stage column increases the acrylic acid concentration from 37 to 84 wt%. The bottoms stream contains 99 wt% water. The second distillation column produces 25,500 kg/hr of market grade (99 wt%) acrylic acid. Table 14 summarizes the key parametric assumptions for the major unit operations for this process.

Table 15 summarizes the overall material and energy intensity data extracted from Aspen results. The distillation columns consume the majority of the natural gas requirement.

TABLE 12 Mass and Energy Intensity: Glycerol to 3-HP

	Distillation	EDI
Energy Inputs	*MMBtu/ ton*	*MMBtu/ ton*
Natural gas	6.2	0.62
Electricity	0.04	10
Material Inputs	*ton/ton*	*ton/ton*
Glycerol	2.1	2.2
Na_2HPO_4	0.10	0.11
Arabinose	0.06	0.07

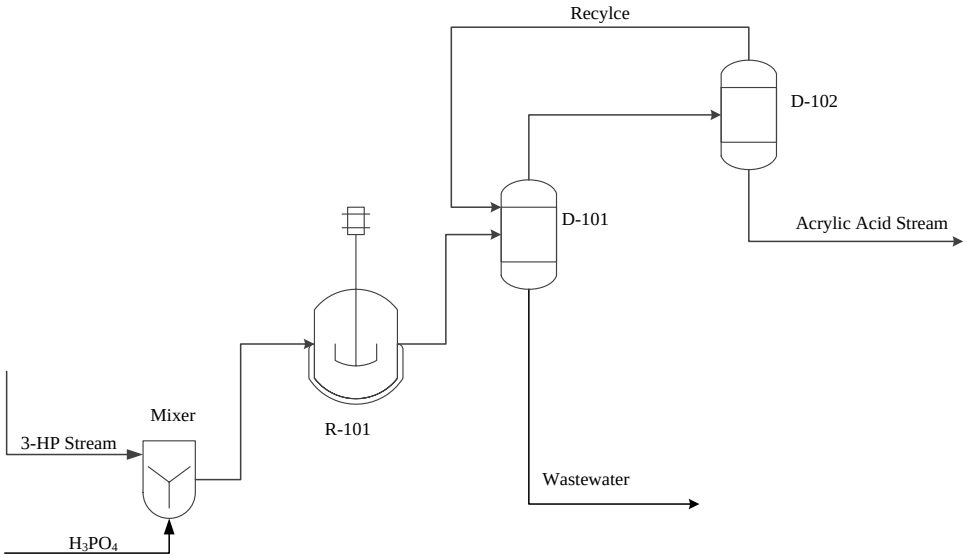

FIGURE 5 Simplified Process Flow Diagram for 3-HP to Acrylic Acid

TABLE 13 Summary of Assumed Stoichiometric Reactions and Yields for Acrylic Acid to 3-HP Process

	Reaction	Reactant	Percent converted to product (by mass)
1	3-HP + 0 H_3PO_4 → Acrylic acid + H_2O	3-HP	80

TABLE 14 Summary of Parameters Used in Key Unit Operations

Unit operation	Aspen Plus ID	Modeling parameters
Stoichiometric reaction-1	RSTOIC	Pressure: 1 bar Temperature: 300°C
Distillation column (D-101)	RadFrac	Condenser pressure: 0.5 bar Stages: 20 Molar reflux ratio: 5×10^{-5} Bottoms to feed ratio: 0.7
Distillation column (D-102)	RadFrac	Condenser pressure: 1 bar Stages: 10 Molar reflux ratio: 0.001 Bottoms to feed ratio: 0.5

TABLE 15 Mass and Energy Intensity: 3-HP to Acrylic Acid

Energy Inputs	*MMBtu/ton*
Natural gas	0.98
Electricity	3.0×10^{-4}
Material Inputs	*ton/ton*
Glycerol	1.3

4.5 3-HYDROXYPROPIONIC ACID TO 1,3-PROPANEDIOL

The feedstock for this process, diagramed in Figure 6, is 6,500 kg/hr of 30 wt% 3-HP produced from algal glycerol as described in Section 4.3. The main steps in this process are 1,3-PDO synthesis via hydrogenation, product recovery, and purification.

To begin, 3-HP, water, and ethanol are mixed and pressurized to 102 bar and subsequently heated from 36°C to 104°C before entering the reactor (R-101) for the hydrogenation reaction. Conditions for the reaction are based on a Cargill patent (Meng et al. 2006). The patent reports a new process for hydrogenating 3-HP in the liquid phase in the presence of a ruthenium catalyst to produce 1,3-PDO. n-Propanol and acrylic acid are co-produced. In the process simulation, the hydrogenation reaction consumes 276 kg/hr of pressurized (103 bar) hydrogen. The stoichiometric reactions and yields used in modeling the reaction are summarized in Table 16.

The effluent from R-101 is flashed (Flash-101). The vapor phase effluent from Flash-101 is cooled to about 20°C and sent to another separator (SEP-101), modeled as the component separator unit operation in Aspen Plus. The vapor phase exiting SEP-101 is mainly H_2, which is pressurized and recycled to R-101. The liquid phase output from SEP-101 is mixed with the liquid phase output from Flash-101 and sent to the recovery and purification section, which consists of three distillation columns (D-101, D-102, and D-103). Two of these columns are needed to purify 1,3-PDO to market grade purity (99 wt%). Small amounts of n-propanol (a co-product), 3-HP, and acrylic acid exit column D-103. The process design does not include additional separation processes to recover these compounds because the steps may be economically unviable. The full burden of all process inputs and emissions are therefore attributed to 1,3-PDO. 1,3-PDO is produced at a rate of 1,425 kg/hr. Key parameters and major unit operations for this process are summarized in Table 17.

Table 18 summarizes the overall material and energy intensity for this design process obtained from Aspen Plus. The main natural gas consumers (70%) are the distillation columns.

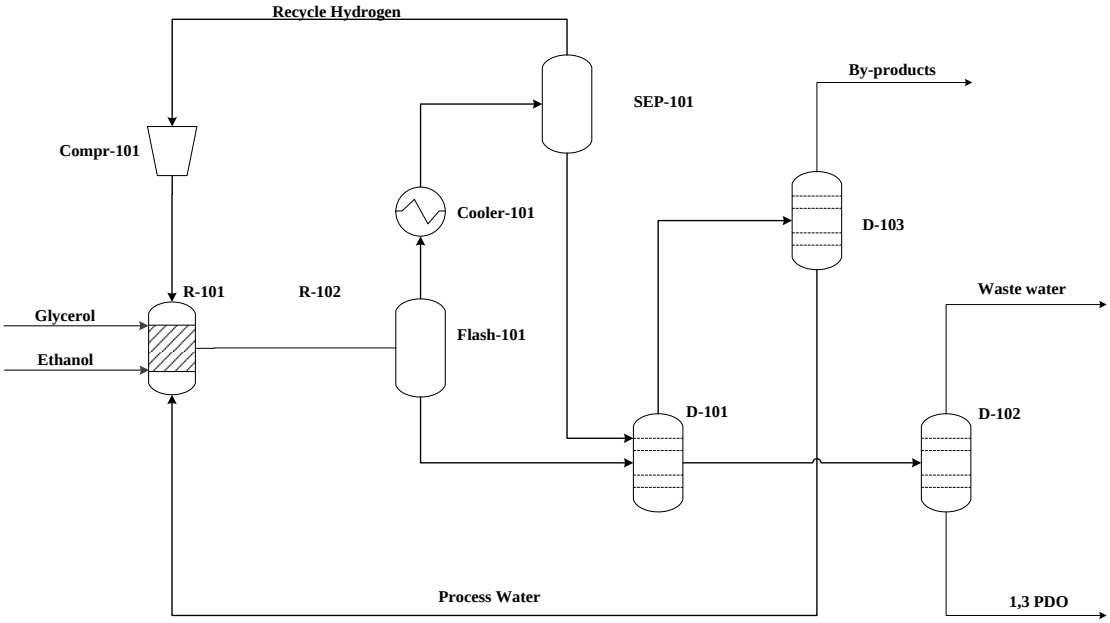

FIGURE 6 Simplified Process Flow Diagram for 3-HP to 1,3-PDO

TABLE 16 Summary of Assumed Stoichiometric Reactions and Yields

	Reaction	Reactant	Percent converted to product (by mass)
1	3-HP + 2 H_2 → 1,3-PDO + H_2O	3-HP	60
2	3-HP → Acrylic acid + H_2O	3-HP	4.0
3	3-HP + 3 H_2 → n-Propanol + 2 H_2O	3-HP	1.0

4.6 CORN STOVER TO CLEAN SUGARS

Humbird et al. (2011) describe an Aspen model for the biochemical production of ethanol from corn stover. We adopted the front end of the model, through hydrolysis, as the process model for production of clean sugars from corn stover. A simplified process flow diagram for this process is shown in Figure 7.

Our assumptions for this process align with those of Humbird et al. Key assumptions are a 2,000 dry ton corn stover/day basis and a 20% stover moisture content. Briefly, corn stover is mixed with hot water and preheated with steam before passing into the pretreatment reactor (R-101) where acid catalyst and more steam are added to drive the pretreatment reaction. After pretreatment, the hydrolysate is conditioned using an NH_3/water mixture in another reactor (R-102) to raise the pH from ~1 to ~5 before the saccharification with cellulase. Humbird et al. (2011) detail the pretreatment and saccharification processes.

TABLE 17 Summary of Parameters Used in Key Unit Operations

Unit operation	Aspen Plus ID	Modeling parameters
Reactor (R-101)	RSTOIC	Pressure: 103 bar Temperature: 150°C
Distillation column (D-101)	RadFrac	Condenser pressure: 1 bar Stages: 12 Molar reflux ratio: 1.5 Distillate rate: 2,979 kg/hr
Distillation column (D-102)	RadFrac	Condenser pressure: 1 bar Stages: 15 Molar reflux ratio: 1.3 Distillate rate: 7,437 kg/hr
Distillation column (D-103)	RadFrac	Condenser pressure: 1 bar Stages: 12 Molar reflux ratio: 0.4 Distillate rate: 136 kg/hr
Compressor	Compr	Isentropic Pressure: 103 bar Stages: 3

TABLE 18 Mass and Energy Intensity: 3-HP to 1,3-PDO

Energy Inputs	*MMBtu/ton*
Natural gas	41
Electricity	1.5
Material Inputs	*ton/ton*
3-HP	1.3
H_2	0.06

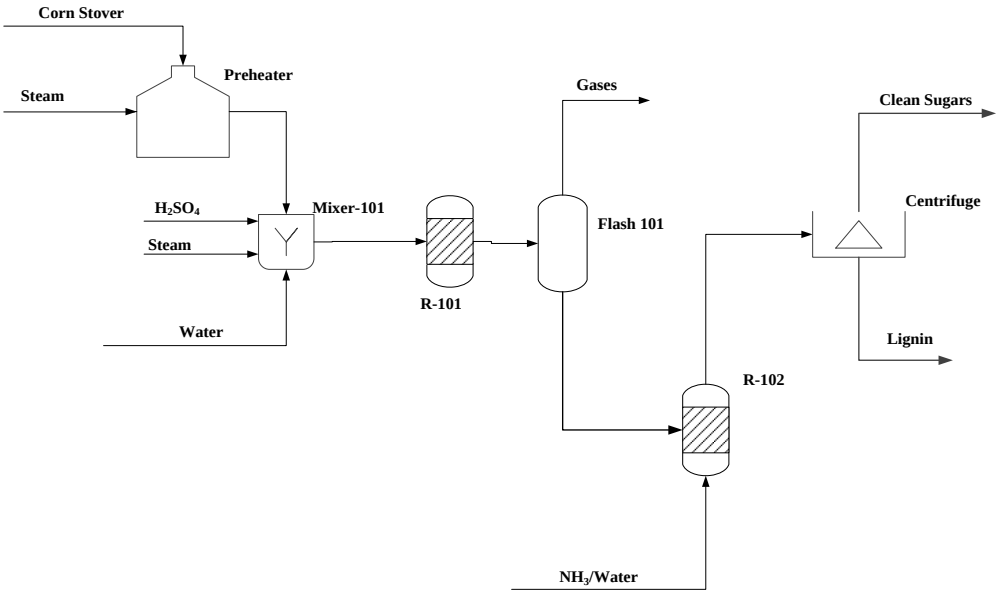

FIGURE 7 Simplified Process Flow Diagram for the Conversion of Corn Stover to Clean Sugars

After saccharification, the clean sugar product stream is centrifuged to remove solid residues such as cell mass, lignin, and undegraded polymeric sugars. We assume electricity is co-produced from excess heat generated onsite and displaces grid electricity. The sugar-rich slurry from the centrifuge, produced at a rate of 69,400 dry kg/hr, serves as the clean sugar feedstock for the production of both succinic acid and isobutanol. The composition of the clean sugar product stream is summarized in Table 19.

Finally, the overall material and energy intensity for this process is summarized in Table 20. About 90% of the natural gas demand is consumed to meet the steam requirement for the pretreatment reaction. Heating the reactor consumes the rest.

4.7 CLEAN SUGARS TO ETHYLENE

Haro et al. (2013) conducted a technoeconomic analysis of the production of ethylene, considering two key technologies, i.e., dehydration of bioethanol and co-production via the methanol-to-olefins (MTO) pathway. The former was adopted in our analyses. The authors constructed process flow diagrams using Aspen to generate the mass and energy flow balances. They considered several routes to ethanol including biochemical processing (enzymatic hydrolysis), thermochemical processing (both direct and indirect syntheses from syngas), and hybrid processing (fermentation of syngas) of biomass. We averaged Haro et al.'s material and energy intensity results for the different ethanol-to-ethylene pathways, which were similar, and adopted this average value in GREET. Table 21 summarizes the averaged material and energy intensity for ethanol to bioethylene.

TABLE 19 Clean Sugars Composition

Components	Mass fraction (wt%)
Water	83.51
Ethanol	0.00
Glucose	6.99
Galactose	0.28
Mannose	0.12
Xylose	3.88
Arabinose	0.47
Glucooligomer	0.33
Galactooligomer	0.01
Mannaoligomer	0.00
Extract	3.05
Soluble lignin	0.15
Hydroxymethylfurfural	0.09
Furfural	0.08
Lactic acid	0.01
NH_4SO_4	0.59
$NH_4CO_2CH_3$	0.44
Oil	0.00

TABLE 20 Mass and Energy Intensity: Corn Stover to Clean Sugars

Energy Inputs	*MMBtu/ton*
Natural gas	1.8
Electricity	0.19
Material Inputs	*ton/ton*
Corn stover	1.5
NH_3	0.02
Cellulase	0.20
H_2SO_4	0.03

TABLE 21 Mass and Energy Intensity: Ethanol to Bioethylene

Energy Inputs	*MMBtu/ton*
Natural gas	2.2
Electricity	1.1
Material Inputs	*ton/ton*
Corn stover	1.7

4.8 CLEAN SUGARS TO SUCCINIC ACID

The production of succinic acid from clean sugars proceeds as illustrated in Figure 8. Feedstock sterilization, fermentation, and product separation and recovery are the dominant process steps.

This process takes as input 69,400 dry kg/hr clean sugars, which are produced as described in Section 4.6. We adopted thermodynamic properties for the components of the clean sugar stream (Table 19) from Wooley and Putsche (1996).

Prior to fermentation, the clean sugar stream is mixed with the fermentation media, which is mostly corn steep liquor (CSL). For feedstock sterilization, the mixed stream is heated from 30°C to 121°C for about 15 minutes and subsequently cooled to the fermentation temperature.

We modeled fermentation of the sterilized sugar stream with *Actinobacillus succinogenes* (*A. succinogenes*) *CGMCC1593* based on data from Zheng et al. (2009),who report that this organism uses both glucose and xylose to produce succinic acid. For the fermentation process, we assumed a residence time of 48 hr and a fermentation temperature of 37°C. Nitrogen sources for *A. succinogenes* were CSL and diammonium phosphate (DAP). The assumed fermentation reactions are summarized in Table 22. After fermentation, the broth is flashed to purge the fermentation gases. Subsequently, centrifugation separates the cell mass from the liquid product stream, which is sent to the purification section.

Two separation scenarios were investigated for the product recovery and purification. While Scenario 1 investigated succinic acid recovery via LLE; Scenario 2 adopted EDI unit operation. Scenario 1 includes vacuum distillation, crystallization, and drying with low-pressure nitrogen. Scenario 2 replaces LLE and the low-pressure nitrogen dryer with an EDI unit and centrifuge.

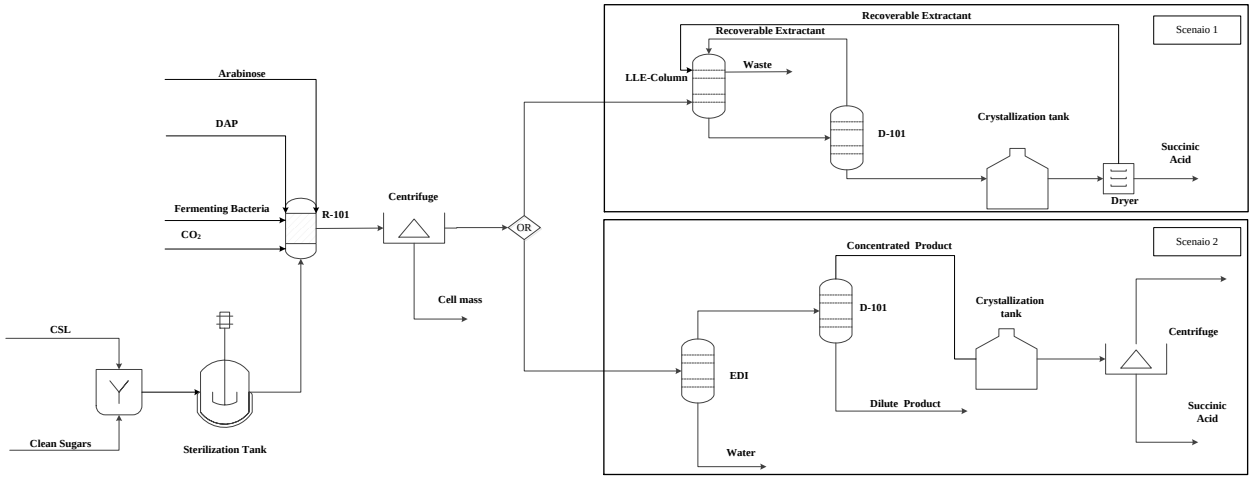

FIGURE 8 Simplified Process Flow Diagram for Clean Sugars to Succinic Acid

TABLE 22 Summary of Assumed Stoichiometric Reactions and Yields

	Reaction	Reactant	Percent converted to product (by mass)
1	Glucose + 2 CO_2 → 2 Succinic acid + O_2	Glucose	81
2	Glucose → 2 Lactic acid	Glucose	0.1
3	Glucose → 3 Acetic acid	Glucose	0.03
4	Glucose + 0.018 DAP + 0.3704 Protein → 6 *Z. mobilis* + 2.4 H_2O	Glucose	0.02
5	3 Xylose + 5 CO_2 → 5 Succinic acid + 2.5 O_2	Xylose	81
6	Xylose → 2.5 Acetic acid	Xylose	0.03
7	Xylose + 0.015 DAP + 0.3087 Protein → 5 *Z. mobilis* + 2 H_2O	Xylose	0.02

Data from Huh et al. (2006) guided the design of the LLE column in Scenario 1. In the column, tri-n-octylamine (TOA) is the extractant. A diluent (1-octanol) is needed, however, because TOA is highly viscous. We assumed that the concentration of TOA in 1-octanol is 9 wt% and that the extractant and diluent will be recovered from subsequent processing steps and recycled. We assumed that the LLE column recovers 100% of the succinic acid in some residual broth. This mixture is pumped to a 20-stage vacuum distillation column. The succinic acid-rich stream from distillation is crystallized at 4°C. Next, the product enters a low-pressure N_2 dryer to drive off residual moisture. The dryer output is 36,600 kg/hr of pure succinic acid crystals. Key parameters for the unit operations in this process with separations as in Scenario 1 are summarized in Table 23.

For Scenario 2, the EDI unit was modeled using the component separator in Aspen Plus. We assumed that 95% of succinic acid in the clarified broth will be recovered at 60 wt% in the

concentrated product effluent of the EDI unit (Lin 2013). This concentrated product stream is further purified using a 20-stage distillation column (D-101) and additional unit operations. We assumed that the EDI unit consumes approximately 2,930 kWh electricity/ton 3–HP (10 MMBtu/ton) (Lin 2013). Key parametric assumptions for the major unit operations are summarized in Table 23. In Scenario 2, we estimated a succinic acid (100%) production rate of 35,200 kg/hr.

This process model adopted several assumptions that need to be further investigated in future work. First, although parameters from Humbird et al. (2011) were used to model bacteria growth, these parameters were not specific to *A. succinogenes*. To improve model accuracy, cell growth parameters specific to this organism should be incorporated into the model. Secondly, our treatment of recovery and recycling of TOA and the diluent is a simplified scenario. More robust treatment of the clean-up of the recycled extractant and diluent stream would provide a better accounting for energy and materials consumed in this process. Finally, modeling of the EDI unit is based on laboratory experience as discussed with Lin (2013). The sensitivity of the results to the assumed electricity consumption of EDI should be investigated because the energy consumption adopted here is not process-specific.

Finally, Table 24 summarizes the overall material and energy intensity for this process.

TABLE 23 Summary of Parameters used in Key Unit Operations

Unit operation	Scenario	Aspen Plus ID	Modeling parameters
Reactor (R-101)	1 and 2	RStoic	Pressure: 1 bar Temperature: 32°C
LLE column	1	Extract	Stages: 20 Thermal option: Adiabatic Pressure: 1 bar
Distillation column (D-101)	1	Radfrac	Condenser pressure: 0.1 bar Stages: 20 Molar reflux ratio: 0.04 Bottoms to feed ratio: 0.1
EDI	2	Component Separator	95% separation efficiency of succinic acid
Distillation column (D-101)	2	Radfrac	Condenser pressure: 0.1 bar Stages: 20 Molar reflux ratio: 0.035 Bottoms to feed ratio: 0.07
Crystallization unit	1 and 2	Crystallizer	Pressure: 1 bar Temperature: 4°C

TABLE 24 Mass and Energy Intensity: Clean Sugars to Succinic Acid

	LLE	EDI
Energy Inputs	*MMBtu/ton*	*MMBtu/ton*
Natural gas	14.0	8.4
Electricity	1×10^{-3}	10
Material Inputs	*ton/ton*	*ton/ton*
Clean sugars	1.90	2.0
DAP	0.02	0.02
CSL	0.12	0.13
Yeast	0.01	0.01

4.9 CLEAN SUGARS TO ISOBUTANOL

Figure 9 shows a simplified process flow diagram of the fermentation of clean sugars to isobutanol. We based this process simulation on Tao et al. (2014).

The feedstock for the process is 69,400 kg/hr of dry clean sugars (Table 19). Prior to fermentation, the clean sugar stream is mixed with CSL, sterilized at 120°C for 15 minutes, then subsequently cooled to the fermentation temperature.

Our modeling of the fermentation step is based on Baez et al. (2011), who reported using an engineered *E. coli* strain to convert sugars to isobutanol with the formation of very few inhibitors. We assumed that fermentation with *E. coli* occurred at 37°C over 48 hr. DAP is added to the fermentation as a nitrogen source. Yields and stoichiometry for each reaction occurring in the reactor are reported in Table 25. As did Tao et al. (2013), we assumed the *E. coli* uses both the xylose and glucose components in the sugar feed stream. We again used cell growth parameters from Humbird et al. (2011) that are not specific to the organism we used in the process model. As with the simulation of succinic acid with *A. succinogenes*, future refinement of this process model could incorporate organism-specific growth parameters.

After fermentation, the broth is flashed (Flash-101). The liquid effluent from Flash-101 is heated from 32°C to 110°C before passing to the vacuum stripper (D-101). The gaseous phase effluent from the D-101 overhead is 8 wt% isobutanol, while the liquid phase effluent from the bottoms has just 1 wt%. The 1 wt% isobutanol stream is recycled into the fermenter.

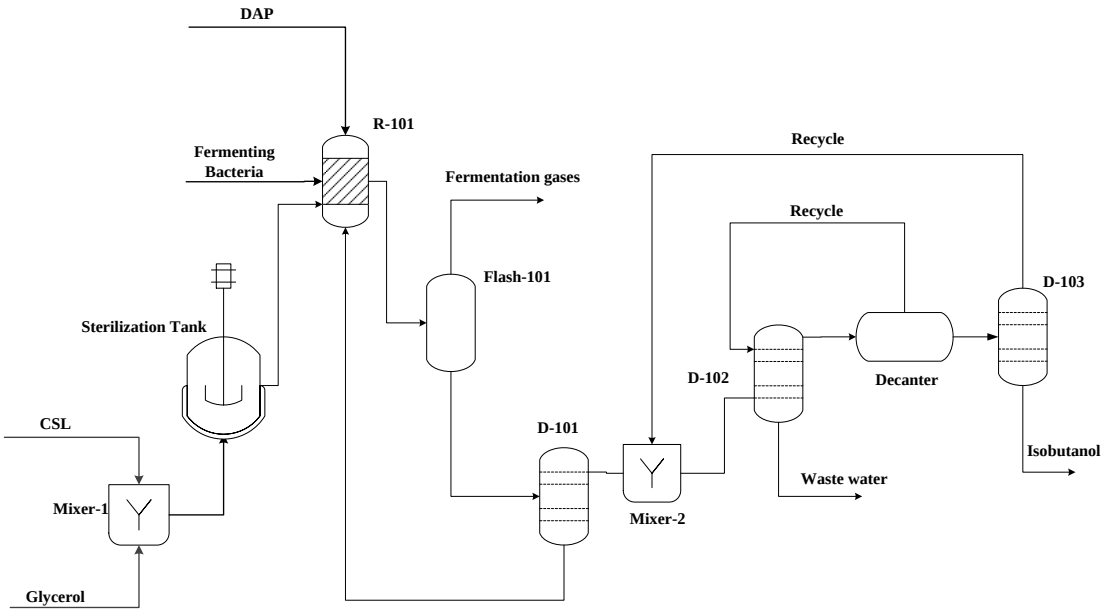

FIGURE 9 Simplified Process Flow Diagram for Clean Sugars to Isobutanol

TABLE 25 Summary of Stoichiometric Reactions and Yields for the Clean Sugars to Isobutanol Process

	Reaction	Reactant	Percent converted to product (by mass)
1	Glucose → Isobutanol + 2 CO_2 +H_2O	Glucose	35
2	6 Xylose → 5 Isobutanol + 10 CO_2 + 5 H_2O	Glucose	35
3	Glucose + 0.018 DAP + 0.3704 Protein → 6 *Z. mobilis* + 2.4 H_2O	Glucose	0.15
4	Xylose + 0.015 DAP + 0.3087 Protein → 5 *Z. mobilis* + 2 H_2O	Xylose	0.15

The concentrated (8 wt%) isobutanol stream is pressurized to 5 bar and heated to 50°C before passing to the second distillation column. The recyclable waste water in the D-102 bottoms is recycled to the fermenter; the liquid overhead stream is a water-isobutanol mixture. This stream is decanted to further concentrate the isobutanol before the rectification tower (D-103). The dilute stream from the decanter is recycled back to D-102. The effluent from D-103 is cooled and recycled to the mixer (T-101). These recycle loops maximize product recovery. The key parametric assumptions for the major unit operations in this simulation are summarized in Table 26. This facility produces approximately 16,000 kg/hr (100 wt%) isobutanol.

Table 27 summarizes the overall material and energy intensity for this process. The distillation columns consume the bulk (92%) of the process natural gas demand.

TABLE 26 Summary of Parameters used in Key Unit Operations

Unit operation	Aspen Plus ID	Modeling parameters
Stoichiometric reaction-1	RSTOIC	Pressure: 1 bar Temperature: 32°C
Vacuum stripper (D-101)	RadFrac	Condenser pressure: 0.1 bar Stages: 20 Molar reflux ratio: 2.4
Distillation column (D-102)	RadFrac	Condenser pressure: 5 bar Stages: 20 Molar reflux ratio: 5×10^{-5} Bottoms to feed: 0.61 (mass)
Distillation column (D-103)	RadFrac	Condenser pressure: 1 bar Stages: 20 Molar reflux ratio: 0.3 Bottoms to feed: 0.66 (mass)
Decanter (D-101)	Decanter	Pressure: 1 bar Heat duty: 0 MMBtu/hr Component mole fraction: 0.5

TABLE 27 Mass and Energy Intensity: Clean Sugars to Isobutanol

Energy Inputs	*MMBtu/ton*
Natural gas	5.8
Electricity	1.6×10^{-2}
Material Inputs	*ton/ton*
Clean sugars	4.5
Corn steep liquor	7.7×10^{-2}
DAP	8.5×10^{-3}
Protein	5.9×10^{-3}

4.10 SUCCINIC ACID TO 1,4-BUTANEDIOL

1,4-BDO synthesis via hydrogenation and product stream purification are the major sections of the process designed to convert 100 wt% succinic acid to 1,4-BDO (Figure 10).

Succinic acid supplied to the facility is mixed with ethanol (13 kg/hr) and water (8,000 kg/hr). The mixed stream is pressurized and heated to 250°C before entering the stoichiometric reactor (R-101) for 1,4-BDO production via hydrogenation.

The parameters for the reactor design are based on Chung et al. (2012, 2013). The authors investigated the conversion of succinic acid to its derivatives by introducing a palladium-loaded mesoporous catalyst in an autoclave batch reactor using support materials. They reported the formation of 1,4-BDO and other co-products (γ-butyrolactone [GBL], tetrahydrofuran [THF]). In addition to the preheated stream, approximately 300 kg/hr of pressurized hydrogen is supplied to the hydrogenation reactor. Table 28 summarizes the assumed stoichiometric reactions and yields used in the stoichiometric reactor.

After the hydrogenation reaction, a single three-phase separator (Flash-101) removes moisture prior to further downstream processing. Three effluent streams are obtained from Flash-101. First, a gaseous stream containing mostly hydrogen is recycled and compressed (Compr-101) before entering R-101. The second stream, which is essentially waste water, (>97wt% water) undergoes no further processing. The third product stream undergoes further downstream purification.

In the product recovery and purification section, this third stream is first preheated to 57°C and passes through a train of distillation columns (D-101, D-102, and D103) to recover the 1,4-BDO and co-products (GBL and THF). Material and energy consumption were allocated among the co-products on a mass basis. Key parameters and major unit operations for this process are summarized in Table 29.

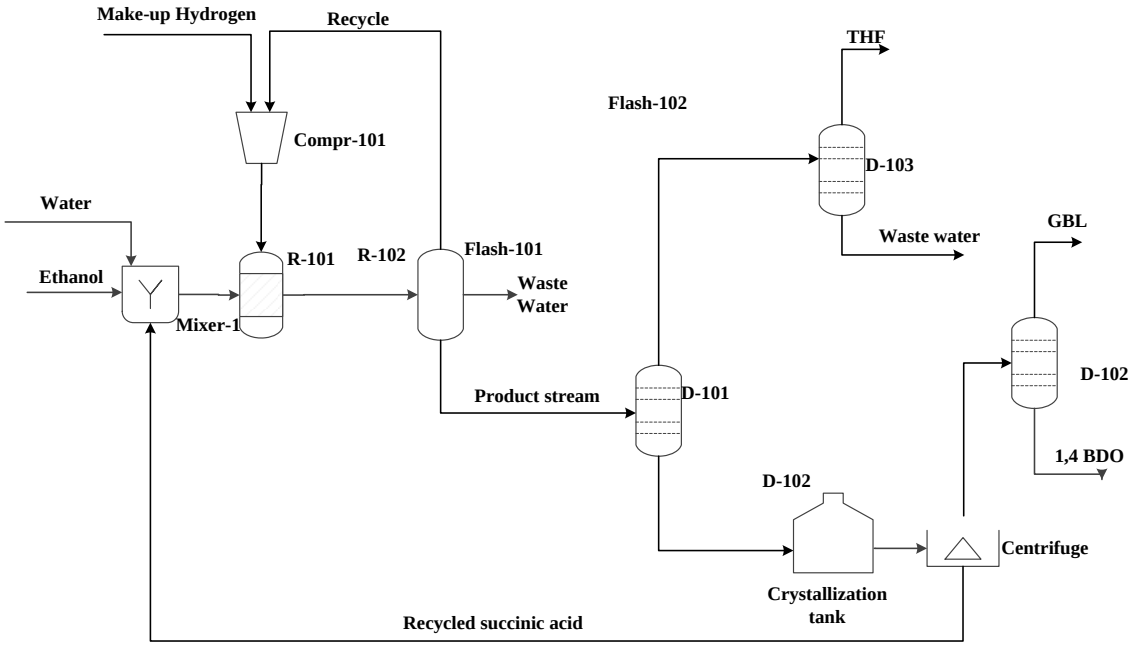

FIGURE 10 Simplified Process Flow Diagram for Succinic Acid to 1,4-BDO

TABLE 28 Summary of Assumed Stoichiometric Reactions and Yields for Biosuccinic Acid to 1,4-BDO

	Reaction	Reactant	Percent converted to product (by mass)
1	Succinic acid + 4 H_2 → BDO + 2 H_2O	Succinic acid	70
2	Succinic acid + 2 H_2 → GBL + 2 H_2O	Succinic acid	1
3	Succinic acid + 4 H_2 → THF + 2 H_2O	Succinic acid	1

TABLE 29 Summary of Parameters Used in Key Unit Operations

Unit operation	Aspen Plus ID	Modeling parameters
Stoichiometric reaction-1	RSTOIC	Pressure: 100 bar Temperature: 250°C
Distillation column (D-101)	RadFrac	Condenser pressure: 2.4 bar Stages: 20 Molar reflux ratio: 0.05 Bottoms to feed ratio: 0.97
Distillation column (D-102)	RadFrac	Condenser pressure: 11 bar Stages: 25 Molar reflux ratio: 0.01 Bottoms to feed ratio: 0.2
Distillation column (D-103)	RadFrac	Condenser pressure: 1.2 bar Stages: 35 Molar reflux ratio: 1×10^{-3} mole Bottoms to feed ratio: 0.92
Compressor	Compr	Isentropic Pressure: 100 bar Stages: 2

Table 30 summarizes the overall material and energy intensity of this process. Operation of the distillation column consumes 88% of the natural gas.

TABLE 30 Mass and Energy Intensity: Biosuccinic Acid to 1,4-BDO

Energy Inputs	*MMBtu/ton*
Natural gas	0.56
Electricity	1.2
Material Inputs	*ton/ton*
Succinic acid	1.3
Ethanol	3.0×10^{-3}

4.11 GLUCOSE OR CLEAN SUGARS TO L-LACTIC ACID

We considered two cases for the production of L-lactic acid. The first case (case 1) involves L-lactic acid production from a pure glucose stream sourced from a corn wet milling facility. In this case, *Lactobacillus lactis* is the fermenting microorganism. In the second case (case 2), we investigated L-lactic acid fermentation using clean sugars produced from corn stover via dilute acid pretreatment assuming *Bacillus coagulans* as the fermenting microorganism.

Yeast extract is a bio-nutrient that can be used in the fermentation step of L-lactic acid production. It provides nitrogenous compounds, carbon, sulfur, trace nutrients, vitamin B complex and other vital growth factors essential for microbial growth (Sigma Aldrich 2015). The Aspen databank does not contain yeast extract among the chemical compounds that can be used in a process. We therefore needed to develop estimates of the composition of yeast extract to use in the Aspen models we developed and describe our approach in Section 4.11.1.

L-lactic acid production process consist of three key sections; ***seed fermentation***, ***fermentation***, and ***downstream separation and purification***. We describe each section of the process simulations in subsections 4.11.2-4.11.4.

4.11.1 Yeast Extract Component Model in Aspen Plus

We reviewed a technical manual on bio-nutrients (BD Bionutrients 2015) to understand the chemical composition of yeast extract. 49 wt. % of yeast extract is made up of free amino acids and peptides, while carbohydrates constitute 12 wt % of yeast extract. Furthermore, ash and sodium chloride (NaCl) constitute roughly 11 wt% of yeast extract. Additionally, hydrosoluble vitamins and fatty acid components are key component of yeast (Jacques et al 2003; Ingledew 2009), the starting feedstock for yeast extract. We assumed that equal amounts of these compounds comprised the balance (28%) of the yeast extract. Figure 11 diagrams the yeast extract composition assumed in the process design.

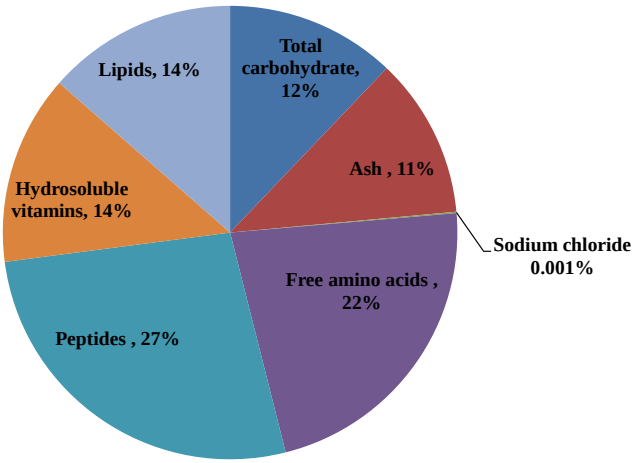

Figure 11: Mass Composition (Dry basis) of Yeast Extract Assumed in this Study

Based on our review of the compositional analysis of yeast extract in the bionutrient technical manual (BD Bionutrients 2015), we estimated the free amino acid profile in yeast extract as in Table 31.

TABLE 31 Summary of Percent Composition of Free Amino Acids in Yeast Extract (Source: BD Bionutrients 2015)

Free Amino Acids	3 Letter Code	Percent Composition (mass basis)
Arginine	Arg	9%
Asparagine	Asn	5%
Aspartic acid	Asp	8%
Cystine	Cys	2%
Glutamic acid	Glu	29%
Glutamine	Gln	1%
Glycine	Gly	5%
Histidine	His	2%
Isoleucine	Iso	9%
Leucine	Leu	16%
Lysine	Lys	10%
Methionine	Met	4%
Total		100%

Peptides are short chains of amino acids that are linked by peptide or amide bonds. We modeled them as free amino acids in Aspen plus based on the chemical composition summarized in Table 32.

TABLE 32 Summary of Percent Composition of Peptides in Yeast Extract (Source: BD Bionutrients 2015)

Free Amino Acids	3 Letter Codes	Percent Composition (mass basis)
Alanine	Ala	10%
Aspartic acid	Asp	11%
Glutamic acid	Glu	60%
Leucine	Leu	9%
Lysine	Lys	10%

Detailed compositional analysis of carbohydrates was not reported in the bionutrient technical manual (BD Bionutrients 2015). We therefore assumed the carbohydrate composition

in *Saccharomyces cerevisiae*, a species of yeast as the carbohydrate distribution profile for yeast extract. This is summarized in Table 33.

TABLE 33 Summary of Percent Composition of Carbohydrate Content in Yeast Extract (Ingledew 2009)

Carbohydrates	Percent Composition (mass basis)
glycogen	21%
trehalose	2%
mannan	32%
glucan	45%
Total	100%

Finally, lipids and hydrosoluble vitamins were modeled as squalene and ascorbic acids which are also key components of yeast (Ingledew 2009).

4.11.2 Seed Fermentation Design

In the seed fermentation section, we modeled the growth of microorganisms and glucose metabolism in the production of inoculum for the production fermenter. Apart from minor differences in the respective growth media composition for *Lactobacillus lactis* and *Bacillus coagulans*, all seed fermentation process assumptions for both microorganisms are identical. The primary stages in this section of the design are sparging of reactors with nitrogen (N_2) gas to create anaerobic conditions and sterilization of nutrients for the preparation of sterile inoculum.

The MRS medium used for growth and maintenance of *L. lactis* contains approximately 45 wt% animal tissues, beef extract and yeast extract as protein sources (Atlas 2010). We made a simplifying assumption that only yeast extract is used as the protein source because we lack life cycle inventory data for animal tissues and beef extract. Similarly although the medium Atlas (2010) describes for growth of *B. cogulans* is 38 wt% yeast extract and peptone, we assumed that the protein source is solely yeast extract. Table 34 summarizes specific growth medium composition assumptions for *L. lactis* and *B. cogulans* adopted in our model.

TABLE 34 Growth Media Composition Assumptions

Composition	***L. Lactis*** (Acumedia 2010)	***B. Coagulans*** (ATCC 2015)
Yeast extract	45%	38%
Glucose	38%	29%
Sodium acetate	9.0%	15%
Potassium phosphate	4.0%	1.4%

Dipotassium phosphate		1.4%
Ammonium citrate	3.0%	
Magnesium sulfate	0.18%	1.0%
Manganese sulfate	0.89%	0.029%
Calcium carbonate		14%
Sodium chloride		0.029%
Sodium citrate		0.078%
Copper (II) sulfate		0.029%
Cobalt (II) chloride		0.029%
Total	100%	100%

Figure 12 summarizes key unit operations modeled in the production of sterile inoculum for the main production fermenter. Glucose and other nutrients comprising yeast extract and mineral components were sterilized separately to avoid any browning of sugars or Maillard reactions (Heinzle et al. 2007). The glucose stream is heated to 135^{o}C for 2 minutes, before passing through a heat exchanger (HX-1) to exchange heat with effluent from Mixer-1. The glucose stream is further cooled (Cooler-1) before splitting (Splitter-2) into the seed rectors (Seed Reactor 1 and 2).

Uniformly mixed nutrient effluent from Mixer-1 is preheated to about 100^{o}C in HX-1 using the hot glucose stream from Heater-1. The preheated nutrient solution is subsequently heated (Heater-2) to 135^{o}C for 2 minutes before sending to Tank-1 and further cooled (Cooler-2) to the 45^{o}C. Sterile nutrient solution from cooler-2 is subsequently split (Splitter-1) into the seed reactors.

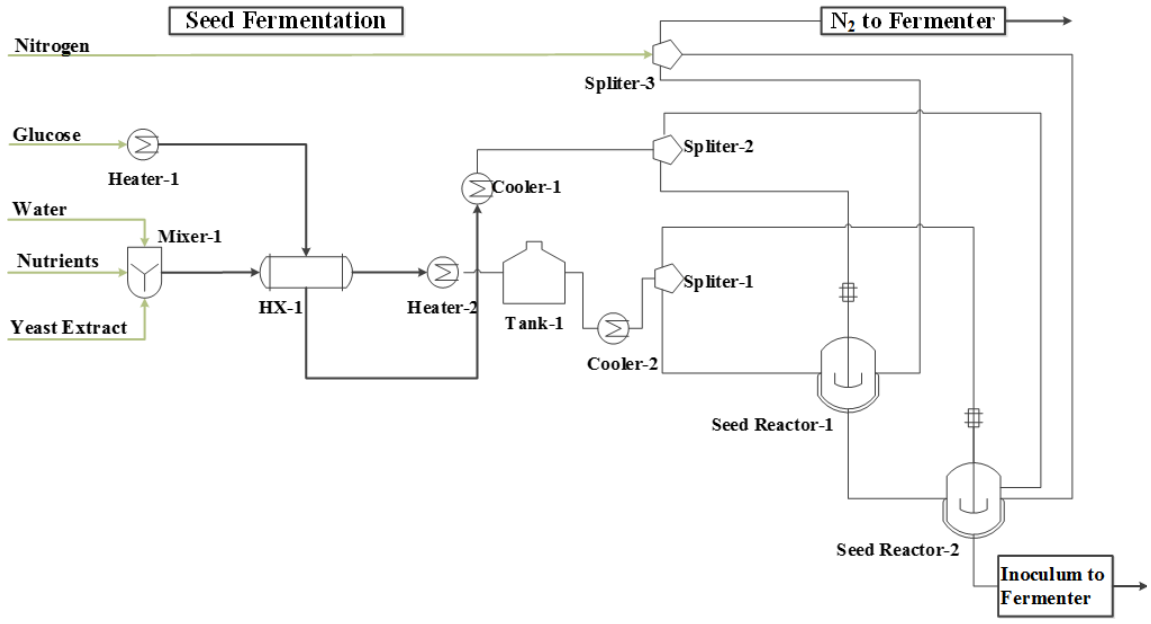

Figure 12 Simplified Process Flow Diagram for Preparation of Fermenter Inoculum

Purchased sterile N_2 (see Figure 12) gas is sparged into seed reactors 1 and 2 to create anaerobic conditions before microbial growth proceeds. We assumed that carbon, vitamins and the nitrogen sources in glucose and yeast extract are primarily used for microbial cell biomass growth while lipids are used for cell maintenance energy (Shuler and Fikret 2002). The reactions we used to model seed reactors 1 and 2 and the associated and conversions are summarized in Table 35.

Readers should note that the reactions reported in Table 35 were developed strictly based on stoichiometry to model cell biomass growth in the seed fermenters. No experimental data were used in their development but if such data become available we will revise our modeling of microbial growth and maintenance.

Finally, specific assumptions for the major unit operations are reported in Table 36.

TABLE 35 Summary of Assumed Stoichiometric Reactions and Yields for Microbial Growth and Maintenance

Rxn No.	Reaction	Reactant	Percent converted to product (by mass)	
			Seed Reactor-1	Seed Reactor-2
1	Arg + Glucose --> 5.1 Biomass + 5.1 CO_2	Glucose	50%	100%
2	Asn + Glucose --> 4.5 Biomass + 4.5 CO_2	Glucose	50%	100%
3	Asp + Glucose --> 4.5 Biomass + 4.5 CO_2	Glucose	50%	100%
4	Cys + Glucose --> 6.0 Biomass + 6.0 CO_2	Glucose	50%	100%
5	Glu + Glucose --> 4.7 Biomass + 4.7 CO_2	Glucose	50%	100%
6	Gln + Glucose --> 4.7 Biomass + 4.7 CO_2	Glucose	50%	100%
7	Gly + Glucose --> 3.7 Biomass + 3.7 CO_2	Glucose	50%	100%
8	His + Glucose --> 4.8 Biomass + 4.8 CO_2	Glucose	50%	100%
9	Iso + Glucose --> 4.5 Biomass + 4.5 CO_2	Glucose	50%	100%
10	Leu + Glucose --> 4.5 Biomass + 4.5 CO_2	Glucose	50%	100%
11	Lys + Glucose --> 4.7 Biomass + 4.7 CO_2	Glucose	50%	100%
12	Met + Glucose --> 4.7 Biomass + 4.7 CO_2	Glucose	50%	100%
13	Lipid + Vitamins --> 13 CO_2 + H_2O	Lipid	50%	100%

TABLE 36 Summary of Parameters Used in Key Unit Operations

Unit Operation	Aspen Plus ID	Modeling Parameter
Heat Exchanger (HX-1)	HeatX	Flow Direction : Countercurrent Minimum temperature approach : 10^oC

Reactor (Seed Reactor-1)	RSTOIC	Temperature : 42^{o}C Pressure : 1 bar
Reactor (Seed Reactor-2)	RSTOIC	Temperature : 42^{o}C Pressure : 1 bar

4.11.3 Fermentation

In this section, pure glucose or the clean sugar stream from acid pretreated corn stover is converted to L-lactic acid and biomass via microbial fermentation. *L. lactis* is the fermenting microorganism when the fermentation media is a pure glucose stream; *B. Coagulans* is used in the case of clean sugar stream. The primary stages involved in the fermentation section are sterilization of supplementary nutrients, sparging of production fermenter with N_2 gas, and the addition of inoculum to the fermenter for the fermentation process.

Glucose and clean sugars from wet corn milling and pretreatment facilities, respectively, would have been subjected to a number of high temperature processes. We therefore treat them as sterile process inputs and do not subject them to any high-temperature sterilization steps like those the nutrients in the model undergo.

Figure 13 diagrams the fermentation process for L-lactic acid using either a pure glucose stream or a clean sugar stream. The supplementary nutrients stream from Mixer-2 was sterilized by preheating it to about 118^{o}C in HX-2 for less than 3 minutes. It is then subsequently brought to ~135^{o}C and sent to Tank-3. The effluent from Tank-3 (sterile nutrient stream) is cooled to about 40^{o}C before transferring to the production fermenter. The production fermenter is sparged with N_2 gas to create anaerobic conditions before introducing the fermentation media.

Before fermentation starts, inoculum from the seed fermenters is loaded at 10 vol% of the production fermenter along with nutrients and other fermentation media. After the addition of the inoculum, fermentation proceeds in a batch mode for 3 days (Walsh and Venus 2013; Yang et al. 2015). However, because LAB is generally inhibited by low pH, $CaCO_3$ is added to the fermenter to maintain a pH of 5.5-6.5 resulting in the formation of calcium lactate in the production fermenter. About 8 wt. % of calcium lactate in the fermentation broth is sent to the purification section to recover free lactic acid.

In Table 37, we summarize the assumed stoichiometric reactions and conversions in the production fermenter. L-lactic acid conversions are based on findings reported by Walsh and Venus 2013; and Yang et al. 2015. Additionally, specific assumptions for the major unit operations in Figure 13 are reported in Table 38.

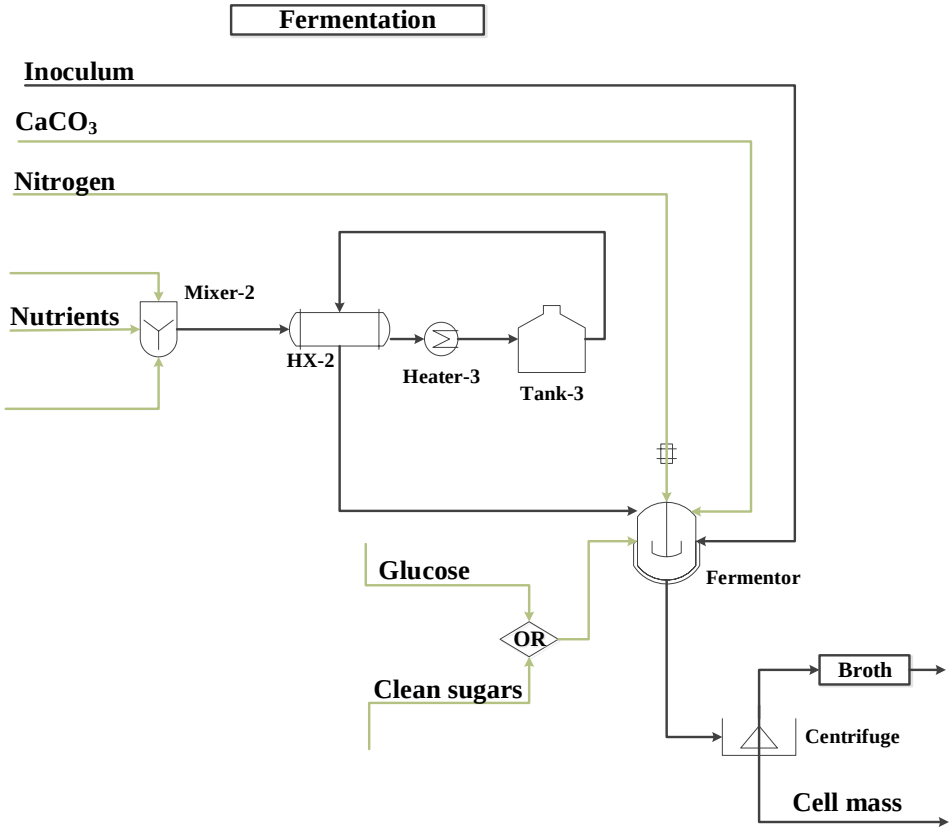

Figure 13 Simplified Process Flow Diagram of Fermentation Process

TABLE 37 Summary of Assumed Stoichiometric Reactions and Yields for Microbial Growth and Maintenance in Production Fermenter

Rxn No.	Reaction	Reactants	Percent converted to product (by mass)	
			L lactis (Pure glucose stream)	*B Coagulans* (Clean sugar stream)
1	Glucose --> 2 L-lactic acid	Glucose	98%	98%
2	3Xylose --> 5 L-lactic acid	Xylose	0%	95%
3	3 Arabinose --> 5 L-Lactic acid	Arabinose	0%	95%
4	Galactose --> 2 L-Lactic acid	Galactose	0%	95%
5	Mannose --> 2 L-Lactic acid	Mannose	0%	95%
6	1.5 L-lactic acid + $CaCO_3$ --> Ca-Lactate + H_2O	L-lactic acid	100%	100%
7	Glycogen --> 26 Biomass	Glycogen	100%	100%
8	Trehalose --> 13 Biomass	Trehalose	100%	100%
9	Mannan --> 6.3 Biomass	Mannan	100%	100%
10	Glucan --> 6.3 Biomass	Glucan	100%	100%
11	0.067 Ala + 0.40 Arg --> 2.7 Biomass + 0.17 CO_2	Ala	85%	85%
12	0.30 Asn + 0.49 Asp + 0.062 Cys + 0.075 Gln + 1.7 Glu --> 15 Biomass + 0.13 CO_2	Asn	90%	90%
13	0.59 Gly + 0.097 His + 0.56 Iso + 0.97 Leu + 0.55 Lys + 0.21 Met --> 14 Biomass + 0.11CO_2	Gly	90%	90%
14	Lipid + Vitamins --> 13 CO_2 + H_2O	Lipid	100%	100%
15	0.30 Asn + 0.49 Asp + 0.062 Cys + 0.075 Gln + 1.7 Glu --> 15 Biomass + 0.13 CO_2	Asn	90%	90%
16	0.59 Gly + 0.097 His + 0.56 Iso + 0.97 Leu + 0.55 Lys + 0.21 Met --> 14 Biomass + 0.11CO_2	Asn	90%	90%
17	0.067 Ala + 0.40 Arg --> 2.68 Biomass + 0.17 CO_2	Aln	10%	10%

TABLE 38 Summary of Parameters used in Key Unit Operations for Corn starch-derived L-lactic acid

Unit Operation	Aspen Plus ID	Modeling Parameter
Heat Exchanger (HX-2)	HeatX	Flow Direction : Countercurrent Minimum temperature approach : 10^{o}C
Reactor (Fermenter)[a]	RSTOIC	Temperature : 42^{o}C Pressure : 1 bar
Reactor (Fermenter)[b]	RSTOIC	Temperature : 50^{o}C Pressure : 1 bar

[a] Fermentation reactor assumptions for *L. lactis*, corn starch-derived glucose

[b] Fermentation reactor assumptions for *B. coagulans* cellulosic biomass-derived clean sugars

4.11.4 Product Separation and Purification

In this section of the process, calcium lactate in the fermentation broth chemically transforms to crude dilute lactic acid, which is subsequently separated and purified to polymer-grade L-lactic acid. We based the development of this portion of the process model on two studies (Barve et al. 2010; Bapat et al. 2014). The design consists of three primary stages. First, we model the chemical transformation of calcium lactate to dilute crude lactic acid and calcium sulfate. The second stage involves the production of methyl lactate and water via esterification in a counter-current reactive distillation column (RDC). The third and final stage involves the hydrolysis of pure methyl lactate to high purity L-lactic acid.

Figure 14 summarizes the product separation and purification section for L-lactic acid. For the first stage of this process, the fermentation broth containing about ~8 wt% of calcium lactate reacts with H_2SO_4 in Reactor-1 resulting in the formation of dilute crude L-lactic acid and calcium sulfate. The solid-liquid effluent from Reactor-1 is passed through a centrifuge to separate L-lactic acid from calcium sulfate solids. Using a falling film evaporator (FFE), crude dilute lactic acid is concentrated to about 50 wt% before it is sent to the RDC. We adopted a series of flash tanks to model the FFE to concentrate the L-lactic acid solution because Aspen plus does not contain FFE units. In case 1, only two flash tanks were needed to reach the ~50 wt% L-lactic acid concentration effluent from the FFE. However, three flash tanks were required in case two to reach the same L-lactic concentration. This stems from differences in supernatant stream composition from centrifuge (see Figure 14). While it is predominantly crude L-lactic acid in case 1, there are additional impurities in the clean sugar stream in addition to the crude L-lactic acid in case 2. These impurities (e.g. ammonium sulfate, ammonium acetate) modeled as soluble solids are components of the stover-derived-sugar stream (Adom et al., 2014a). The effluent from the FFE containing about 50 wt% L-lactic acid is passed to the RDC.

In the second stage, the L-lactic acid stream from the FFE is sent to the countercurrent RDC to react (see Figure 14) with methanol in an equilibrium reaction producing methyl lactate and water by means of esterification. The liquid overhead stream from the RDC is sent to a distillation column (Dist-4) to recover residual methanol which is recycled back to the RDC. To concentrate the methyl lactate liquid effluent from the bottom of the RDC, the stream is passed through two fractional distillation columns (Dist-1 and Dist-2). This process concentrates the methyl lactate liquid effluent (~40 wt. %) from the RDC to about 90-95% before sending to the third stage of the separation process.

The final and third stage of the process involves production of high purity L-lactic acid via hydrolysis of methyl lactate and a subsequent distillation step. The concentrated methyl lactate stream from Dist-2 is passed into a hydrolysis reactor (Reactor-2) where it undergoes hydrolysis using pure lactic acid as an auto-catalyst. In addition to accelerating the rate of reaction the auto-catalyst aids in the production of high purity L-lactic acid (Bapat et al. 2014). Effluent from Reactor-2 is sent to Dist-3 to recover pure L-lactic acid (99 wt%) and the overheads byproduct sent to Dist-4 to recover residual methanol.

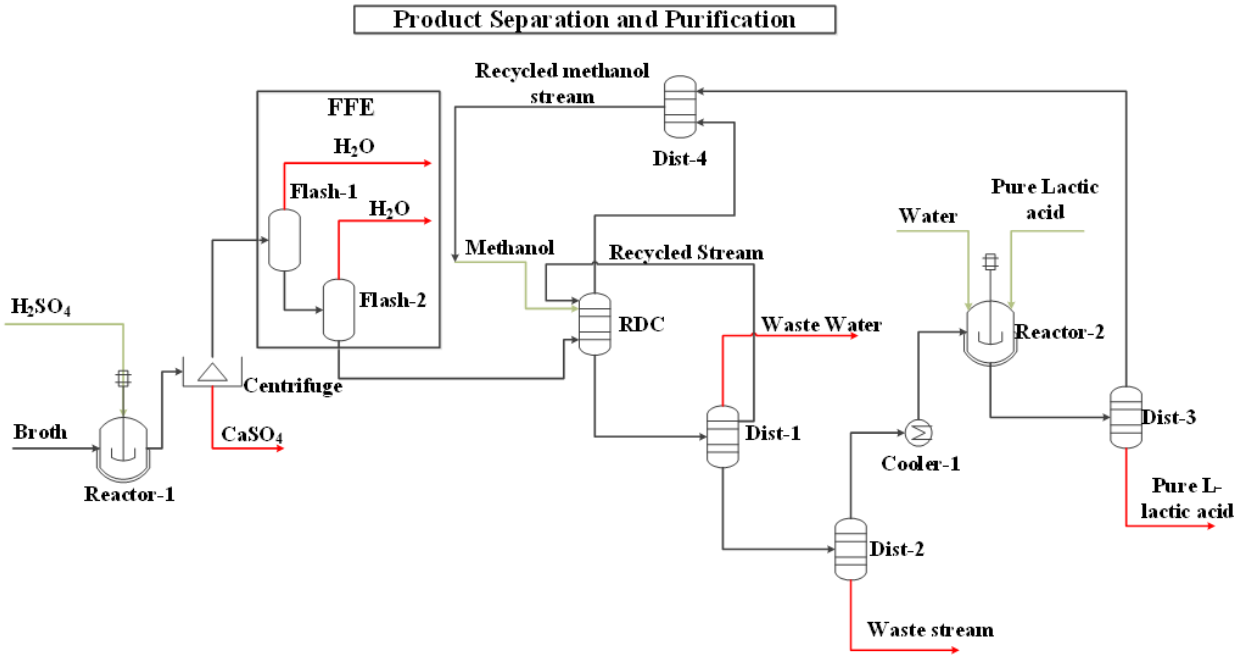

Figure 14 Simplified Diagram of the Product Separation and Purification Process

Specific parametric assumptions for the major unit operations in the process simulations are summarized in Table 39.

TABLE 39 Summary of Parameters used in Key Unit Operations for Corn stover-derived L-lactic acid

Unit Operation	Aspen Plus ID	Modeling Parameter		
		Parameter	**Case 1**	**Case 2**
Reactor (Reactor-1)	RSTOIC	Temperature (^{o}C) Pressure (bar)	30 1	30 1
Flash Tank(Flash-1)	Flash-2	Duty (MMbtu/hr) Pressure (drop): (bar)	0 3.1	0 -0.55
Flash Tank (Flash-2)	Flash-2	Temperature : (^{o}C) Pressure (drop): (bar)	112 -2	131 -0.1
Flash Tank (Flash-3)	Flash-2	Temperature : (^{o}C) Pressure (drop): (bar)		192 -0.1
Column (RDC)	RadFrac	Condenser pressure: (bar) Stages Reflux ratio (mass) Distillate-to-feed ratio (Mass)	1 20 0.15 0.46	1 20 0.15 0.46
Column (Dist-1)	RadFrac	Condenser pressure: (bar) Stages Reflux ratio (mass) Distillate-to-feed ratio (Mass)	2 10 0.44 0.15	2 10 0.49 0.15
Column (Dist-2)	RadFrac	Condenser pressure: (bar) Stages Reflux ratio (mass) Distillate to feed ratio (Mass)	1 10 0.05 0.15	1 10 0.1 0.502
Column (Dist-3)	RadFrac	Condenser pressure: (bar) Stages Reflux ratio (mass) Distillate to feed ratio (Mass)	0.1 15 0.1 0.42	0.1 15 0.01 0.35
Column (Dist-4)	RadFrac	Condenser pressure: (bar) Stages Reflux ratio (mass) Distillate to feed ratio (Mass)	0.1 10 0.005 0.85	0.1 10 0.005 0.95
Reactor (Reactor-2)	RSTOIC	Temperature (^{o}C) Pressure (bar)	30 1	30 1

Table 40 summarizes the overall material and energy intensity for the L-lactic acid process. Data reported in Table 40 reflects the 80% natural gas-fired boiler efficiency needed to meet plant heat demand.

TABLE 40 Summary of Material and Energy Intensity Flow for L-lactic acid

	Case 1 (Corn-derived)	**Case 2 (Corn stover derived)**
Total Energy Input :	*MMBtu/ton*	*MMBtu/ton*
Natural gas	16	17
Electricity	0.0058	0.027
Mass Inputs	*ton/ton*	*Ton/ton*
Ammonium citrate	0.025	0.0038
Calcium carbonate	0.96	1.01
Dipotassium phosphate		0.00081
Mono potassium phosphate	0.0020	0.00083
Glucose	1.3	0.01
L-lactic acid	0.010	0.0097
Manganese sulfate	0.0048	0.0012
Magnesium sulfate (kieserite)	0.0012	0.000049
Methanol	0.035	0.0099
Nitrogen gas	0.099	0.1
Sodium acetate	0.064	0.018
Sodium chloride	0.12	0.019
Sulfuric acid	0.94	0.94
Yeast extract	0.34	0.33
Sodium citrate		0.000044
Cobalt (II) chloride		0.0000024
Copper (II) sulfate		0.000022
Clean sugars		1.2

In terms of natural gas and electricity requirements, there was not much difference between the two different design cases examined. Even though case 1 is about 10% more material intensive than case 2, they are comparable to a very large extent irrespective of the type of feedstock usage i.e., clean sugars or glucose (see Table 40). The largest contributor (52-58 wt%) to material consumption is the use of ancillary compounds such as such as sulfuric acid and methanol. Feedstock consumption was the next largest contributor ranging from 32-34 wt%. Nutrient consumption ranged from 9-15 wt%, with case 1 being more nutrient intensive.

Finally, gypsum produced from the fermentation process was assumed to be of little value and therefore considered as a waste for disposal (Meng et al. 2012; Vaidya et al. 2005).

4.12 L-LACTIC ACID TO ETHYL LACTATE

Ethyl lactate is produced commercially via a reversible esterification of lactic acid with ethanol; water is a by-product. We provide detailed descriptions of the continuous process simulation developed using Aspen Plus and document key parametric assumptions such as reaction kinetics, unit operation process conditions, and separations process parameters adopted for our simulations of ethyl lactate in the following subsections.

4.12.1 Reversible Esterification Process

In this section a mixture of pure ethanol and L-lactic is converted to ethyl lactate via a reversible esterification process (Figure 15) in a Plug Flow Reactor (PFR) reactor. After the conversion process, two sieve distillation columns are used together with a pervaporator to produce market grade ethyl lactate while recovering residual ethanol and L-lactic acid for recycling.

The esterification process uses Amberlyst 15, a commercial acid resin catalyst (Delgado et al. 2010). We did not include consumption of this catalyst in the process model or subsequent analysis because of insufficient data on catalyst lifetime and composition. Lactic acid can undergo self-polymerization into dimers and trimers and potentially impact yield in the conversion process. Delgado et al. (2010) reported about 3.1 wt% (dimers and trimers) in commercial monomeric lactic acid at about 50wt%. As a result, L-lactic self-polymerization could potentially occur in the feed stream for ethyl lactate production; however, this was excluded from our Aspen Plus model to simplify the simulation process.

Ethyl lactate process was modeled in Aspen Plus with the UNIQUAC thermodynamic property method as diagrammed in Figure 15.

Equimolar amounts of pure ethanol and L-lactic acid are thoroughly mixed to ensure a uniform ethanol/L-lactic acid mixture before the mixture enters the PFR (see Figure 15). A reversible esterification reaction between the reactants proceeds at approximately 95^{o}C. The PFR liquid effluent contains about 76 wt% ethyl lactate, 12 wt% water, residual ethanol and L-lactic acid and is sent to a sieve distillation column (DIST-1). Due to the azeotropic behavior of the water/ethanol mixture, a stream containing these two compounds exits DIST-1 via the overhead vapor stream as distillate while higher concentrations of ethyl lactate together with residual L-lactic acid are recovered from the bottom liquid stream. The distillate from DIST-1 is sent to a pervaporator to further recover ethanol, which is recycled into the PFR. Given that Aspen Plus does not contain a pervaporator unit operation, we modeled the pervaporator in Aspen Plus using the component separator unit operation. We could not then use Aspen Plus to estimate the energy consumed in this unit operation, but estimated it instead with data from Kosaric et al. (2000). The liquid effluent from DIST-1 is further distilled in another sieve distillation column (DIST-2) to recover market-grade ethyl lactate in the overhead stream. The residual L-lactic acid in the bottom stream is recycled into the PFR.

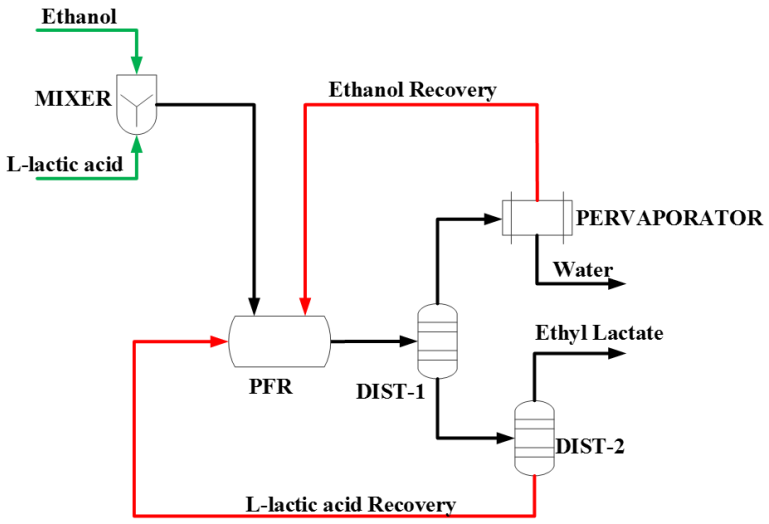

Figure 15 Simplified Process Flow Diagram for Ethyl Lactate Reversible Esterification Process

One key consideration in the parametric specification for DIST-2 in Aspen Plus was to ensure that the overhead stream temperature was below the degradation temperature of ethyl lactate. Specific parametric assumptions for the major unit operations in the process simulations are summarized in Table 41.

TABLE 41 Summary of Parameters used in Key Unit Operations (Data Source: Adams and Seider (2008))

Unit Operation	Aspen Plus ID	Modeling Parameter	
Reactor (Reactor-1)	PFR RPLUG	Pre-exponential factor Activation energy (kcal/mol) Temperature (^{o}C)	0.020 7.3 95
Column (Dist-1)	RadFrac	Condenser pressure: (bar) Stages Reflux ratio (mole) Boilup ratio	1 13 18 12
Column (Dist-2)	RadFrac	Condenser pressure: (bar) Stages Reflux ratio (mole) Boilup ratio	0.51 13 0.5 7
Pervaporator	SEP	98% separation efficiency of ethanol	

In Table 42, we summarize the energy consumed in the production of ethyl lactate.

TABLE 42 Summary of Material and Energy Intensities for ethyl lactate

Energy Input	*MMbtu/ton*
Natural gas[a]	8.2
Electricity[a]	0.051
Material Inputs	*ton/ ton*
L-lactic acid	0.81
Ethanol	0.42

[a]Pervaporation consumes 4% and 99% of the total natural gas and electricity consumption in Table 42.

Electricity constitutes less than 1% of energy consumption, which is dominated by the use of natural gas for heating. Consumption of L-lactic acid and ethanol accounted for 66 and 34% of material consumption, respectively.

5 MATERIAL AND ENERGY FLOW DATA FOR CONVENTIONAL PRODUCTS

Material and energy flow data for conventional products were drawn from the literature. Data sources included journal articles, technical reports, and one industry report. In several instances (e.g., propylene oxide, adipic acid, acrylic acid), we relied on process simulation results from journal articles. In the case of propylene glycol, no material and energy flow data were available to our knowledge, so we developed our own Aspen simulation to estimate these data. One important data source was Franklin Associates (2011). In this report, material and energy flow data from many key petroleum-derived and other chemicals are reported with clear explanations of how co-product accounting was handled. In many cases, industry sources provided and reviewed the data in this 2011 report. In the following sections, we detail data sources, calculation methodology, assumptions, and GREET input data for each of the conventional products considered in the GREET model.

5.1 PROPYLENE GLYCOL

Figure 16 lays out the pathway for the production of conventional propylene glycol. Material and energy flow data for production of propylene from refined petroleum products and natural gas were derived from a 2011 report from the American Chemistry Council (Franklin Associates 2011). In this process, hydrocarbons and steam are cracked in a furnace at 1000°C. We used GREET data for liquefied petroleum gas (LPG) for the raw material refined petroleum products, which can include ethane, propane, liquid feed, heavy raffinate, and diesel natural gas (DNG). In addition to natural gas, the process also consumes small amounts of electricity, gasoline, and diesel. Eighty-five percent of the natural gas is used as a process feedstock. The remaining 15% is used to generate process energy.

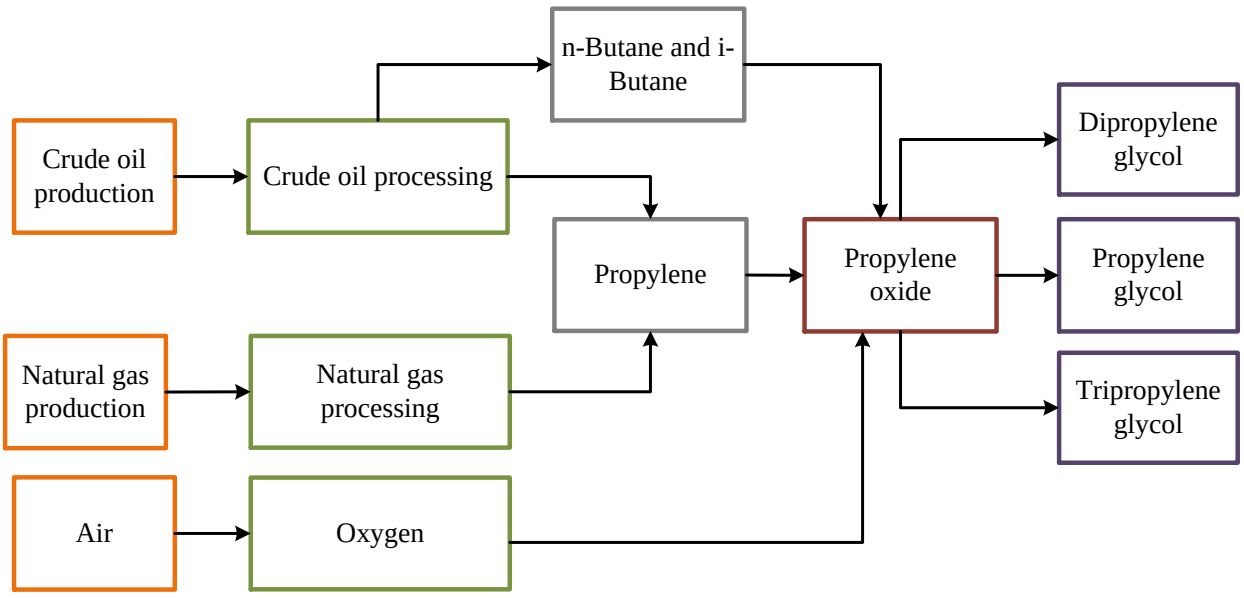

FIGURE 16 Conventional Production of Propylene Glycol

The production of propylene oxide has been modeled as a two-stage process by Ghanta et al. (2013), and we use their results in GREET. The first stage is isobutane oxidation. Isobutane, n-butane (both of which are treated as LPG in GREET), and oxygen are the feeds to this stage. Small amounts of methanol and acetone are produced. In the second stage—the propylene epoxidation stage—propylene oxide, crude tert-butyl alcohol, and small amounts of methanol and acetone are produced. The process consumes steam and electricity. Sixty-three percent of the latter is used for cooling. Process energy and material inputs are allocated to propylene oxide on the basis of mass.

Propylene glycol is produced from the hydration of propylene oxide. The reaction is uncatalyzed and occurs at 200°C and 15 atm. Co-products include dipropylene glycol, tripropylene glycol, and some higher glycols. To optimize production of monopropylene glycol, the molar ratio of water to propylene oxide is about 15. For each ton of monopropylene glycol, 0.1 tons of dipropylene glycol and 0.01 tons of tripropylene glycol are produced (Chinn and Kumamoto 2011). The impacts of the process are allocated among these three products by mass. In the absence of literature data describing the energy consumption of this process, it was modeled in Aspen Plus with the Peng-Robinson thermodynamic property method as diagrammed in Figure 17.

At the start of the process, propylene (56,600 kg/hr) and water (~203,000 kg/hr) are mixed and pressurized from 1 to 22 bar before passing to the reactor (R-101). The hydration reaction is uncatalyzed and occurs at ~177°C and 22 bar. Table 43 summarizes the assumed stoichiometric reactions and yields in the reactor.

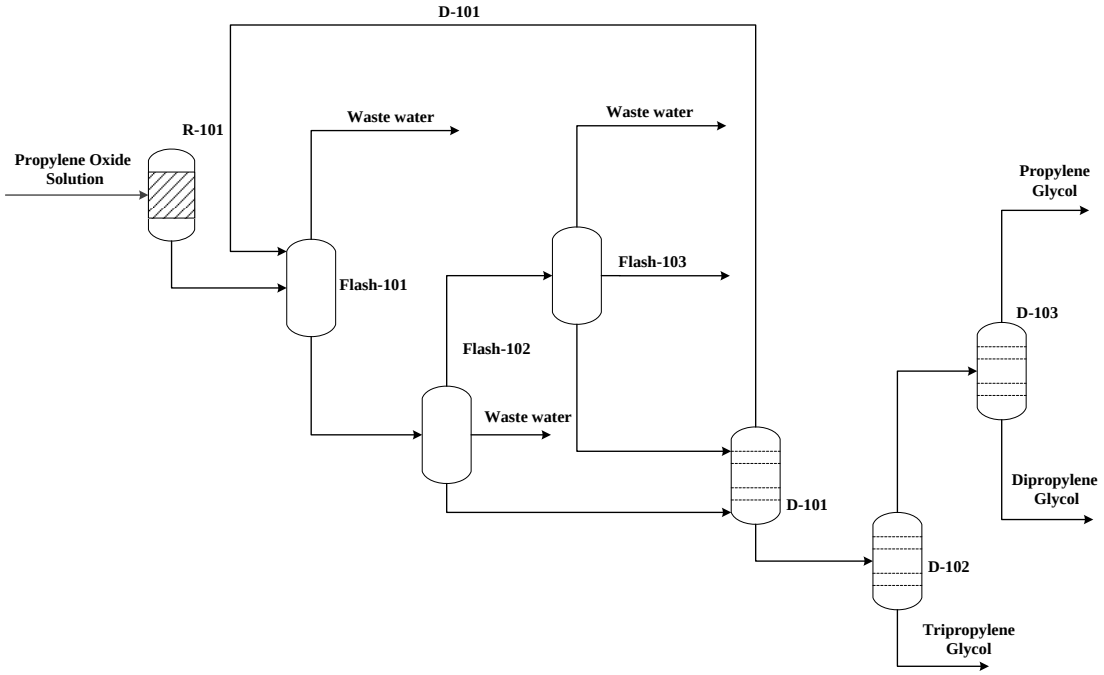

FIGURE 17 Process Flow Diagram for the Production of Propylene Glycol from the Hydration of Propylene Oxide

TABLE 43 Summary of Assumed Stoichiometric Reactions and Yields for Propylene Oxide to PG Process

	Reaction	Reactant	Percent Converted to product
1	Propylene oxide + H_2O → Propylene glycol	Propylene oxide	89.0
2	Propylene oxide + H_2O → Di-propylene glycol	Propylene oxide	0.10
3	Propylene oxide + H_2O → Tri-propylene glycol	Propylene oxide	0.01

Multi-effect evaporators and drying towers are employed to purify the product stream to obtain neat PG. The liquid effluent from R-101 containing PG (25 wt%), dipropylene glycol (2.5 wt%), tripropylene glycol (0.002 wt%), and H_2O (72 wt%) is run through three series of flash tanks (Flash-101, -102, and -103) to recover by-products as well drive off excess water in the product stream. The liquid effluent from Flash-102 and -103 is passed through vacuum distillation columns (D-101, D-102, and D-103) in series to further purify the product stream. Specific design assumptions for the major unit operations are summarized in Table 44. We allocated process inputs among the three co-products on a mass basis.

TABLE 44 Summary of Parameters used in Key Unit Operations

Unit operation	Aspen Plus ID	Modeling parameters
Reactor (R-101)	RSTOIC	Pressure: 22 bar Temperature: 155°C
Distillation column (D-101)	RadFrac	Condenser pressure: 0.1 bar Condenser temperature: 54.4°C Stages: 21 Molar reflux ratio: 1×10^{-4} Bottoms to feed ratio: 0.75
Distillation column (D-102)	RadFrac	Condenser pressure: 0.1 bar Condenser temperature: 54.4°C Stages: 20 Reflux rate: 0.46 kg/hr Bottoms rate: 140,000 kg/hr
Distillation column (D-102)	RadFrac	Condenser pressure: 0.1 bar Condenser Temperature: 54.4°C Stages: 20 Molar reflux ratio: 1 Bottoms Rate : 3,900

Table 45 summarizes the overall material and energy intensity for this process. About 90% of natural gas demand is consumed by the distillation columns and flash tanks. The remainder (10%) is consumed for reactor operation.

TABLE 45 Mass and Energy Intensity: Conventional Propylene Oxide to PG

Energy Inputs	*MMBtu/ton*
Natural gas	11
Electricity	0.01
Material Inputs	*ton/ton*
Propylene oxide	1.1

5.2 1,3-PROPANEDIOL

The pathway for the production of conventional 1,3-propanediol is in Figure 18. As with propylene, we tapped the report from Franklin Associates (2011) to build material and energy flow data for ethylene. In this process, hydrocarbons are thermally cracked in a furnace at 1000°C. Again, we used GREET data for LPG for the raw material refined petroleum products, which can include ethane, propane, liquid feed, heavy raffinate, and DNG. In addition to natural gas, the process also consumes small amounts of electricity, gasoline, and diesel. 85% of the natural gas is used as a process feedstock. The remaining 15% is used to generate process energy.

Similarly, data for ethylene oxide production was sourced from Franklin Associates (2011). In this process, ethylene is oxidized with air or oxygen over a silver catalyst. Approximately 20-25% of the ethylene burns, producing CO_2 and water. In this analysis, we take the midpoint of this range, 23%. We do not include the catalyst in this analysis, however Urban and Bakshi (2009) found the catalyst contributed minimally to the energy and environmental impacts of the ethylene oxide process. We use Franklin Associates data rather than Urban and Bakshi's analysis because Franklin Associates obtained industry data for energy consumption in the ethylene oxide production whereas Urban and Bakshi estimated it.

Syngas as an intermediate product could be derived from different feedstocks including chemicals, like acetylene or from the gasification of other feedstocks such as biomass or natural gas. In this study, coal and natural gas were considered as syngas feedstocks. Table 47 summarizes the mass and energy inputs for syngas production.

Material and energy flow of syngas sourced from natural gas using autothermal reforming is based on a natural gas-to-liquid transportation fuels via Fischer-Tropsch (FT) synthesis report by NETL (DOE and NETL 2013). Briefly, a mixture of natural gas as a feed and recycle gases from the FT processes is sent to a pre-former to convert non-methane hydrocarbons into synthesis gas. Effluent from the pre-former is combined with oxygen and steam and the mixture is subsequently directed into an autothermal reformer (ATR) which represents a process

intensification of synthesis gas production, commercially proven by Haldor-Topsoe (DOE and NETL 2013). One advantage of the ATR technology over traditional processes (steam reforming and partial oxidation) is that it is essentially adiabatic (Zeman et al. 2011).

TABLE 46 Material and Energy Flows in the Production of Conventional Propylene Glycol

	Propylene (Franklin Associates 2011)	Propylene oxide (Ghanta et al. 2013)	Propylene glycol
Energy Inputs (MMBtu/ton)			
Natural gas	31	13	10.
Electricity	0.98	7.1	0.01
Gasoline	5.8×10^{-4}		
Diesel	5.6×10^{-4}		
LPG	14.3	2.1 (butanes)	
Material Inputs (ton/ton)			
Oxygen[a]		0.22	
Propylene		0.15	
Propylene oxide			1.1
Co-products (ton/ton)			
Dipropylene glycol			0.08
Tripropylene glycol			2.6×10^{-4}

[a] Based on NETL report (DOE and NETL 2007).

Material and energy flows during syngas production from coal is based on an NETL report that analyzes a coal-based gas-to-liquids plant (DOE and NETL 2007). To determine the electricity demand for producing syngas, we truncate the NETL process at the point where syngas is produced and sum the electricity demand for all the equipment involved in the process to that point. These include coal handling and milling equipment, a coal slurry pump, slag handling, air separation unit power, compressors for oxygen, syngas, and CO_2 streams, recycle blowers for syngas and tail gas, and auxiliaries for the Selexol and Claus plants that clean the syngas (DOE and NETL 2007). We include the CO_2 emissions from the Selexol H_2S/CO_2 removal step. The report also includes the composition of syngas, which is 85wt% CO and 4.2wt% H_2. The balance of the syngas is mostly Ar, CH_4, N_2, and H_2O.

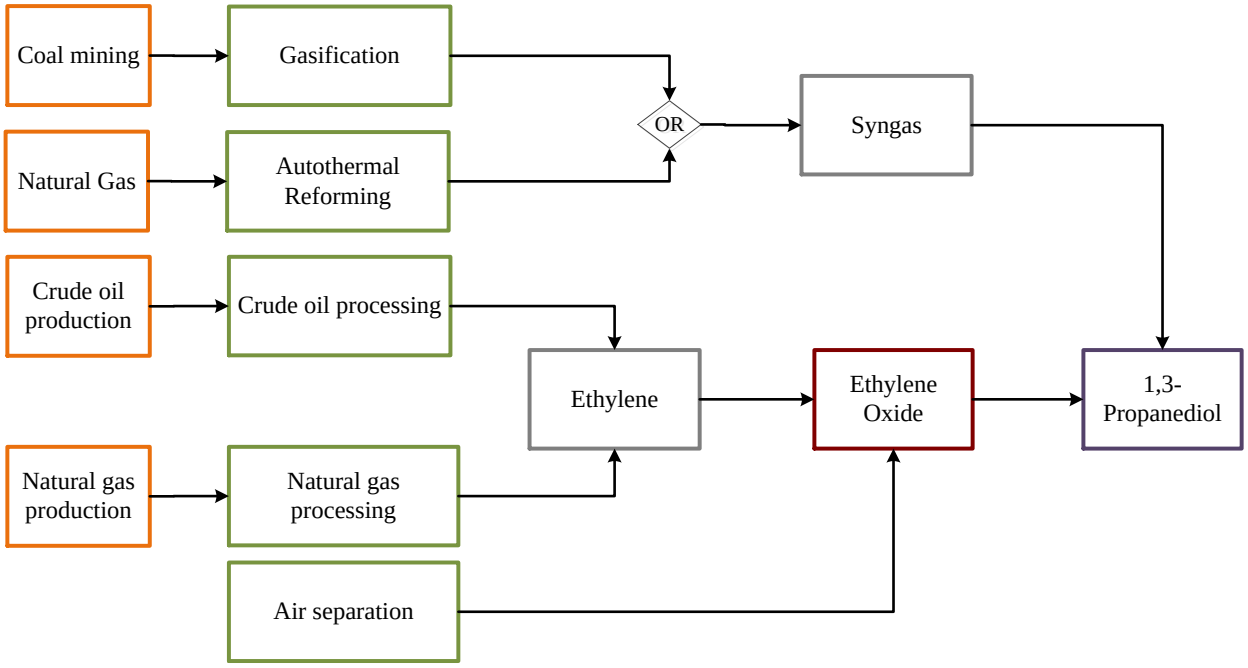

FIGURE 18 Conventional Production of 1,3-Propanediol

Urban and Bakshi (2009) modeled production of 1,3-propanediol with both fossil-based and bio-based feedstocks. We adopt their results for the former in the GREET bioproducts module. They neglected the catalyst in their analysis because insufficient information was available to determine its impact. The key inputs to the process are syngas and ethylene oxide. We calculated the demand for CO and H_2 based on the stoichiometry of the reaction (Equation 1) and determined that H_2 is the limiting reactant. We therefore based the syngas demand on the amount of H_2 the reaction requires and assumed a 50% excess (Urban and Bakshi 2009). The resulting syngas demand is 0.2 ton syngas/ton 1,3-propanediol. The ethylene oxide consumption rate is determined through the stoichiometry of reaction 1 and assuming a 10% excess. The electricity consumed in the PDO process was provided by Urban and Bakshi (2009).

$$C_2H_4O + CO + 2H_2 \rightarrow C_3H_8O_2 \quad (1)$$

Material and energy flows for the production of ethylene, ethylene oxide, syngas, and 1,3-propanediol are summarized in Table 47. Existing GREET data for coal, natural gas, and crude oil production were also used (Burnham et al. 2011, 2014; Cai. et al, 2013).

TABLE 47 Material and Energy Flows in the Production of 1,3-Propanediol

	Ethylene (Franklin Associates 2011)	Ethylene oxide (Franklin Associates 2011)	Natural gas to syngas (NETL 2013)	Coal to syngas (NETL 2007)	1,3-Propanediol (Urban and Bakshi 2009)

Energy Inputs (MMBtu/ton)					
Natural gas	40	3.6	15		
Electricity	0.76	2.1		1.1	32
Gasoline	3.1×10^{-3}				
Diesel	3.0×10^{-3}				
LPG	7.5				
Natural gas used in process[a]	85%				
Process Emissions (g/ton)					
CO_2		520,000			
Material Inputs (ton/ton)					
Ethylene		0.79			
Oxygen		0.88	0.43		
Coal				0.91	
Ethylene oxide					0.64
Syngas					1.9

[a] The balance is combusted in an industrial boiler to produce energy.

5.3 ACRYLIC ACID

Figure 19 diagrams the pathway of conventional acrylic acid production. The raw material is propylene, which, as explained in Section 5.1, is produced from a mix of crude oil products and natural gas.

We extracted material and energy flow data for the conventional production of acrylic acid based on Weigert and Haschke (1976). The conventional process has two main sections, a two-stage vapor phase oxidation reaction section and a separations section. In the reaction section, the heat of reaction is recovered and used to generate steam that is used in the process. Using separate catalysts and two reactors in series, propylene is converted to acrolein in the first reactor and subsequently to acrylic acid in the second reactor. Extraction and distillation columns are used to achieve market grade acrylic acid. In Table 46, we present the energy consumption required to produce propylene. The material and energy demands of producing acrylic acid are presented in Table 48.

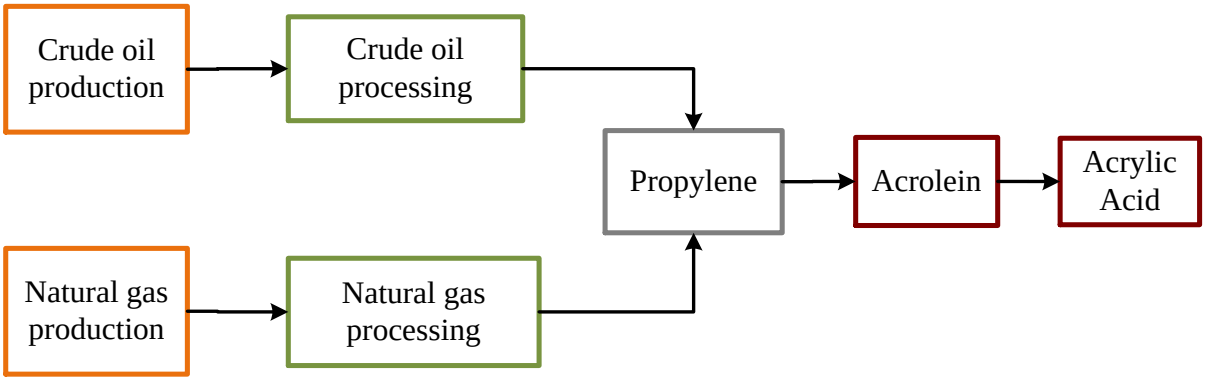

FIGURE 19 Conventional Production of Acrylic Acid

TABLE 48 Material and Energy Flows in the Production of Acrylic Acid

	Acrylic acid (Weigert and Haschke 1976)
Energy Inputs	*MMBtu/ton*
Natural gas	60
Material Inputs	*ton/ton*
Propylene[a]	0.67

[a] See Table 47

5.4 POLYETHYLENE

We will use cradle-to-gate impacts for polyethylene as low-density polyethylene (LDPE) resin as included in the GREET2 model. Data sources and methodology are documented in Keoleian et al. (2011).

5.5 ISOBUTANOL

Isobutanol is generally produced as a by-product of the more desirable isomer, n-butanol, through the reaction of propylene with syngas, as reflected in Figure 20. The products are aldehydes that are then hydrogenated to produce the alcohols. We obtained material and energy flow data for a U.S.-based process to produce isobutanol from a Nexant report (2011). The amounts of raw materials and energy the process consumes are proprietary. Therefore, we report only the final values for energy consumption and air emissions as they are used in the GREET bioproducts module. We allocated the burdens of the process between the two isomers by mass to obtain a result of 254,000 g CO_2e/ton isobutanol.

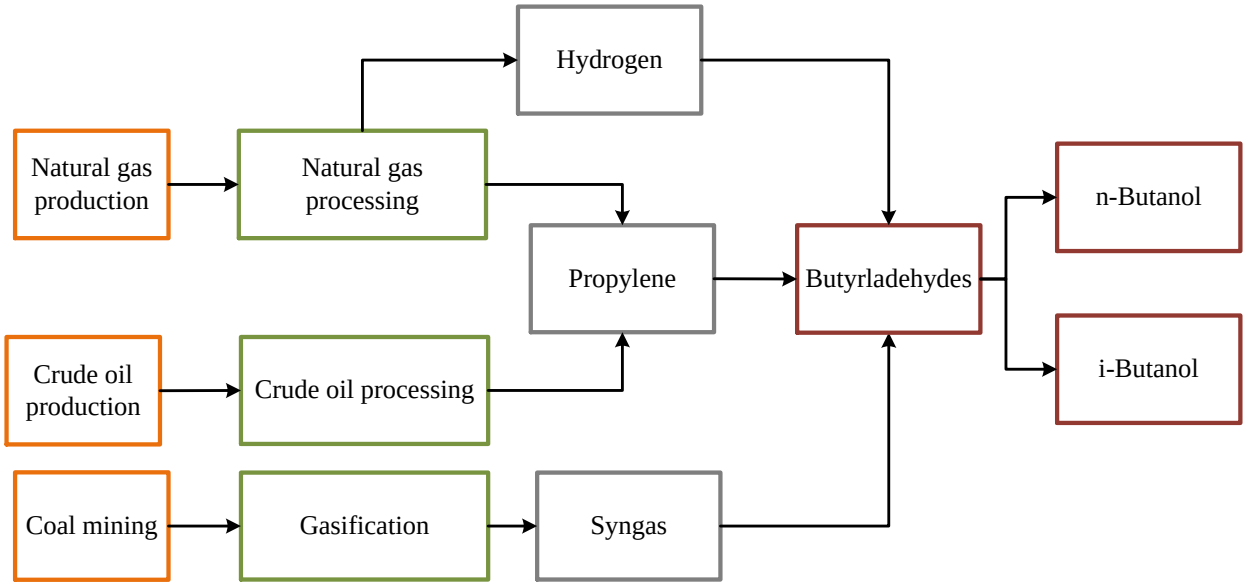

FIGURE 20 Conventional Production of Isobutanol

5.6 1,4-BUTANEDIOL

Currently, the majority of 1,4-butanediol is manufactured by the hydrogenation of butynediol (Haas et al. 2005). This compound is produced in the Reppe process, which takes formaldehyde and gaseous acetylene as feedstocks. The butynediol produced as the intermediate is hydrogenated to produce the final butanediol product. This pathway to conventional 1,4-butanediol is shown in Figure 21.

The first key input to the 1,4-butanediol process is formaldehyde. The raw material for formaldehyde is methanol. It is produced from the steam reforming of light hydrocarbons and subsequent conversion of synthesis gas to methanol. Existing GREET data for the production of methanol were used. Two dominant processes are used to produce formaldehyde from methanol. One uses a metal oxide catalyst; the other a silver catalyst (EC 2003). In both cases, the feedstock is methanol. In the United States, about 59% of formaldehyde plants use the metal oxide catalyst. About 41%, including a major formaldehyde producer, use the silver catalyst. In this analysis, we use the weighted average of parameters for these two processes, which produce an off-gas that can be sent to a catalytic oxidizer for heat recovery. These thermal oxidizers recover about 70% of the heat of these streams (http://www.megtec.com/magnum-catalytic-oxidizer). We assume the recovered steam can replace natural gas combusted in an 80% efficient boiler.

Acetylene is assumed to be produced by the partial oxidation of methane, consuming fossil fuel and electricity (Gannon et al. 2003). One-third of the methane is used as a process feed; the balance is combusted to provide steam (Davis and Funada 2011). Some N-methylpyrrolidinone is used to separate out the acetylene product. The product stream includes H_2 and CO which can be separated as syngas for use in chemical synthesis.

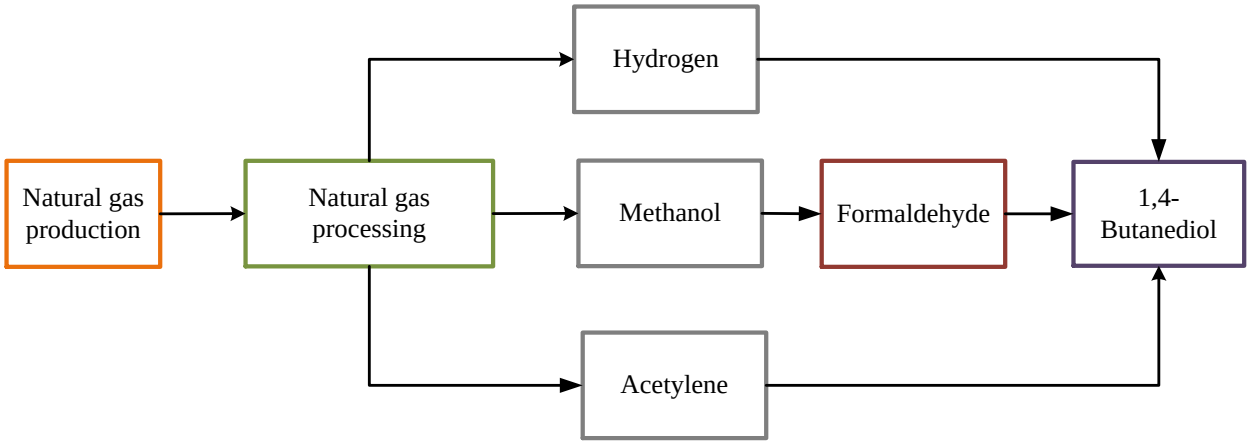

FIGURE 21 Conventional Route to 1,4-Butanediol

The mass fraction of acetylene in the product stream is about 16% (Gannon et al. 2003). We allocated process burdens among co-products on a mass basis. Some process CO_2 emissions form during the partial oxidation reaction (0.12 ton CO_2/ton C_2H_2) by mass allocation. We assume methane in the product stream is recovered and does not constitute a GHG emission. Table 49 summarizes the material and energy consumed in the production of formaldehyde, acetylene, and 1,4-BDO.

TABLE 49 Material and Energy Flow Data in the Production of 1,4-Butanediol

	Formaldehyde[a]	Acetylene (Gannon et al. 2003)	1,4-Butanediol (Evers et al. 1997)
Energy Inputs (MMBtu/ton)			
Natural gas		28 (31% used for product)	0.72
Electricity	0.59[b]	1.2	
Material Inputs (ton/ton)			
Methanol	1.2[c]		
Oxygen		0.82	
Acetylene			0.28
Formaldehyde			0.66
Hydrogen			0.05
N-methylpyrrolidone		0.083	
Co-products			
Steam (MMBtu/ton)	1.8[d]		

[a] Weighted average for silver- and metal oxide-catalyzed processes.
[b] Althaus et al. (2007)
[c] Bizzari (2012)
[d] EC (2003)

5.7 ADIPIC ACID

Adipic acid is produced in a two-step process that consumes cyclohexane, nitric acid, and air (Figure 22).

Cyclohexane is produced from the hydrogenation of benzene. Nickel-based or homogeneous catalysts are used (Zhang et al. 2008). Benzene itself is a building block of the petrochemical industry and can be made by several routes. The reforming of naphtha over a platinum-containing catalyst and the recovery of aromatics from pyrolysis gasoline (pygas) together account for 70% of the world production of benzene (Franklin Associates 2011). The data set used in this analysis for benzene takes both of these routes into account by weighting them according to production (⅓ of production from pygas, ⅔ from naphtha reforming) (Franklin Associates 2011).

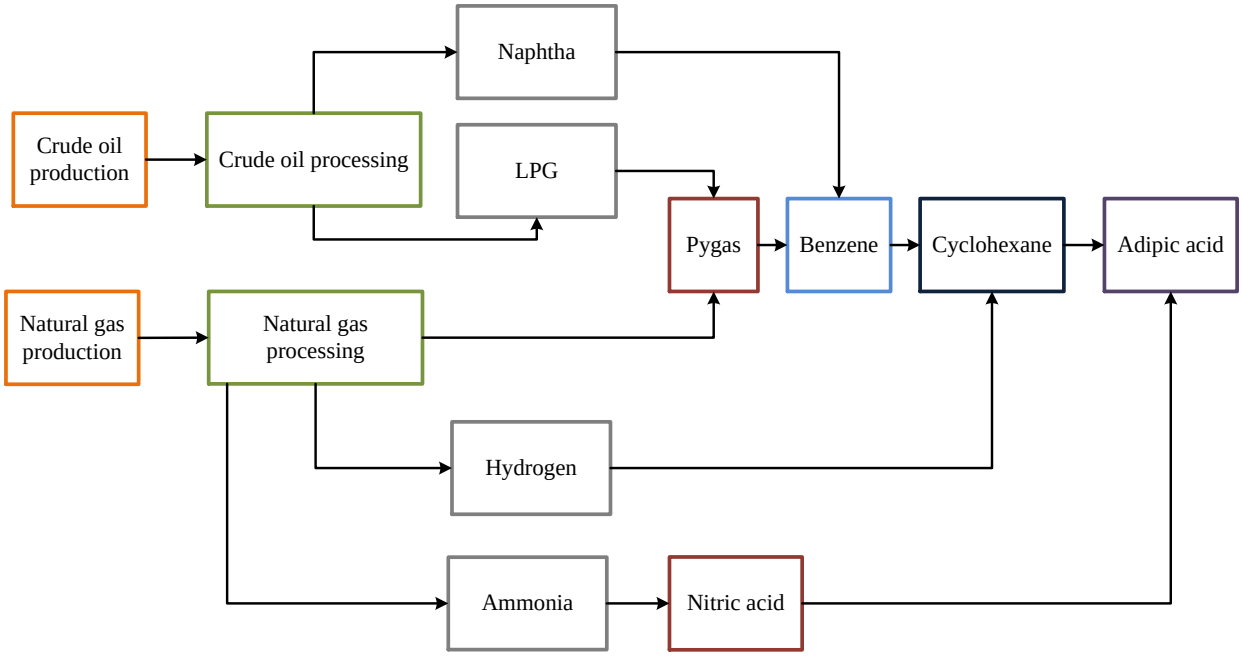

FIGURE 22 Conventional Route to Adipic Acid (Note that the pygas-to-benzene and naphtha-to-benzene routes are separate; benzene can be produced from either raw material.)

Nitric acid is another key input into the adipic acid process. It is used in the second step, in which a mixture of cyclohexanol, an alcohol, and cyclohexanone, a ketone, are oxidized with HNO_3. The ketone-alcohol mixture is generally called a KA oil. During the oxidation of the KA oil, some HNO_3 is converted to NO, NO_2, and N_2O. Some NO and NO_2 can be recovered as HNO_3 through absorption and recycled to the oxidation reactor. N_2O cannot be recovered in this way and is emitted. Given pressure to reduce greenhouse gas emissions from this process, there has been an industry-wide effort to install N_2O abatement technology at adipic acid plants. The World Resources Institute and World Business Council on Sustainable Development (IPCC 2006) provide a calculator to estimate N_2O emissions based on the adipic acid production rate. The calculator uses default Intergovernmental Panel on Climate Change (IPCC) values for N_2O

emissions from adipic acid plants. It allows users to select an N_2O abatement technology, and for each such technology provides an N_2O destruction efficiency and a utility factor. The utility factor represents the percent of time the equipment is running. For this analysis, we chose thermal destruction, which can allow for some heat recovery, because the literature analysis of adipic acid from which we adopted adipic acid production material and energy flow data (Wang et al. 2013a) did not consider energy consumed in abatement processes. The thermal destruction technique will consume energy, but also produce some that can be recovered, so we assume that its net effect on process energy consumption is negligible.

The nitric acid demand in Table 50 reflects a worst-case scenario based on Wang et al. (2013a). If HNO_3 can be recovered from NO and NO_2 in the absorber, the net consumption of HNO_3 could decrease to 0.15 ton/ton. This case will be considered in a sensitivity analysis.

TABLE 50 Material and Energy Flows in the Production of Adipic Acid

	Pygas (Franklin Associates 2011)	Benzene (Franklin Associates 2011)	Cyclohexane (Zhang et al. 2008)	Adipic Acid (Wang et al. 2013a)
Energy Inputs (MMBtu/ton)				
Natural gas	27	1.5	0.25	24
Electricity	1.1	0.15	0.03	
Residual oil		1.3		
Diesel	6.0×10^{-4}	0.13		
LPG	17			
Naphtha		26		
Material Inputs (ton/ton)				
Pygas		0.34		
Benzene			0.94	
Hydrogen			0.14[b]	
Cyclohexane				0.64
Nitric acid				1.4
Nitrous Oxide Process Emissions (kg/ton)				
Nitric oxide				27
Nitrous oxide				9.7[a]

[a] From IPCC calculator assuming thermal destruction.

[b] Hydrogen requirement is based on double the stoichiometric amount.

5.8 ETHYL ACETATE AND N-METHYL-2-PYRROLIDONE

We chose two conventional solvents against which to compare ethyl lactate's life-cycle FEC and GHG emissions. The first, ethyl acetate (EtOAc) is an important organic ester with wide industrial application as a solvent in pharmaceuticals, surface coating and thinners. Primary commercial production of this solvent is via esterification of ethanol and acetic acid (Dutia 2004). EtOAC is very similar structurally to ethyl lactate. It is therefore expected that ethyl lactate could fully substitute for this compound (Patel et al. 2006).

NMP, the second reference solvent, is also an important industrial solvent with applications in petrochemical processing, coatings, and agricultural chemicals (Harreus et al. 2000). Nelson et al. (2011) also reported NMP's application in battery manufacturing process. Commercial production of NMP is carried out via chemical synthesis between γ-butyrolactone (GBL) and excess aqueous methylamine (Harreus et al. 2000). However, because NMP is hazardous to use and produce, there are efforts to find nontoxic and nonhazardous functional substitutes (Reisch 2008). NMP was chosen as the second reference solvent because, it can be substituted with ethyl lactate, which has good solvating properties (Pereira et al. 2011).

Material and energy flow data based on Righi et al. (2011) for EtOAc is summarized in Table 51. Given the lack of publicly available information regarding the material and energy intensity of producing this compound, these authors developed an Aspen simulation to model its production and estimate these intensities. While the authors provide these intensities in the paper, they do not provide the parameters on which they built the Aspen simulation. Further, although the primary commercial route to EtOAc is the esterification of ethanol and acetic acid, the authors may have modeled EtOAC production based on the Tishchencko reaction, which involves direct conversion of ethanol to EtOAc via condensation through an intermediate acetaldehyde (Colley et al. 2005; Logsdon 2000). One reason we think this may be the case is that the authors did not report a consumption rate of acetic acid. Approximately 68% of energy consumption was attributable to electricity consumption and the remainder due to natural gas (Righi et al. 2011). We are not sure why the electricity consumption rate seems to be higher than what we have observed for many chemical conversion processes (Adom et al. 2014b).

TABLE 51 Material Summary of Material and Energy Intensity Flow for EtOAc (Source : Righi et al., 2011))

Energy Inputs	*MMbtu/ton*
Natural gas	5.1
Electricity	11
Material Inputs	*ton per ton*
Ethanol	1.5

Table 52 summarizes the material and energy flow intensity of NMP and associated production chemical inputs. Dunn et al. (2012b) reported the energy consumption requirement for NMP production. In this effort, we have expanded this data set to include the consumption of GBL and methylamine reported by Lammens et al. (2011). They investigated the life-cycle

impacts of producing four compounds (N-methylpyrrolidone, N-vinylpyrrolidone, acrylonitrile, and succinonitrile) sourced from sugar beet vinasse-derived glutamic acid, an amino acid from a low-value byproduct.

TABLE 52 Summary of Material and Energy Intensity Flow for NMP

Energy Input	NMP (Dunn et al. 2012b; Lammens et al. 2011) - *MMbtu/ton*	GBL (Javaid and Bildea 2014) - *MMbtu/ton*	Methylamine (Righi et al. 2011) - *MMbtu/ton*
Natural gas	1.7	0.7	8.0
Electricity	1.0		0.07
Mass Inputs	*ton per ton*	*ton per ton*	*ton per ton*
γ-Butyrolactone	0.914		
Methylamine	0.33		
Ammonia			0.56
Methanol			1.1
1,4-Butanediol		1.1	

To complete the material and energy flows in the supply chain of NMP, we used material and energy consumption data for the production of GBL and methylamine from Javaid and Bildea (2014) and Righi et al. (2011) respectively. Javaid and Bildea (2014) reported the heat requirement to drive the vapor phase endothermic catalytic dehydrogenation of 1,4-butanediol (BDO) to GBL (0.7 MMbtu/ton). Unfortunately this reference did not include energy consumption associated with downstream separation and purification of GBL. Our energy consumption estimate in Table 53 therefore excludes this energy. As a result, our estimate for energy consumed in producing NMP is likely too low, although the resulting comparison with bio-derived ethyl lactate would then be a worst case result. We used stoichiometry to estimate the material consumption in this process. For the fossil-derived 1,4-BDO input, we used data reported by Dunn. et al (2014).

Finally, using Aspen Plus to model the conversion of ammonia and methanol to methylamine, Righi et al. (2011) estimated the material and energy consumption requirements to produce methylamine. These requirements were adopted in this study.

6 RESULTS FOR BIO-BASED AND CONVENTIONAL PRODUCTS

The material and energy flow data for the bioproducts reported in Section 4 and for conventional products reported in Section 5 have been compiled in the GREET bioproducts module. This module uses existing GREET data for energy sources (e.g., natural gas, electricity) and process inputs (e.g., corn stover, algae, yeast extract) to calculate cradle-to-gate and cradle-to-grave energy consumption, air emissions, and GHG emissions results for each bioproduct and conventional product (Adom et al, 2015; Dunn, et al 2014; Wang et al. 2013; Wang 2014). Cradle-to-gate and cradle-to-grave analyses frame the life cycle of bioproducts differently. In the cradle-to-gate scenario, the analysis is limited to the feedstock production and conversion stages. The cradle-to-grave scenario adds in the end-of-life stage. For reporting of GHG emissions, we assume that the bioproducts and conventional products degrade entirely at end of life, releasing the CO_2 they contain. If the bioproduct is combusted to recover energy, the carbon it contains will still be emitted as CO_2. It is possible that some bioproducts like polyethylene may take over a century to degrade. If the time horizon for the analysis is selected to be less than 100 years, only a portion of the carbon within this product may reach the atmosphere. If the bioproduct (or fossil product) sequesters all or a portion of the carbon it contains, the bioproduct will show an increased GHG reduction as compared to the fossil product because of a GHG credit to the bioproduct from atmospheric carbon uptake during biomass growth.

Cradle-to-grave GHG emissions for the bioproducts and their fossil-based counterparts are displayed in Figure 23. Note that we did not analyze a fossil-based route to 3-HP. In the figure, the green diamonds show the percent reduction associated with the bioproduct as compared to the conventional, fossil-derived compound.

All bioproducts in Figure 23 that have a fossil-based counterpart for comparison exhibited reduced cradle-to-grave GHG emissions reductions ranging from 27% to 86%. In many cases, natural gas and feedstock consumption during conversion drove the overall cradle-to-grave results for bioproducts. For example, comparing 1,3-PDO production from glycerol and 3-HP provides an example of the pivotal role of natural gas input to the conversion process. Three times more natural gas is consumed when 1,3-PDO is produced using the 3-HP feedstock as compared to using the glycerol feedstock. Emissions from the latter pathway are three times lower. The bioproduct with the greatest GHG reductions is biosuccinic acid. Its fossil-based benchmark is adipic acid. Current adipic acid production emits N_2O, a potent greenhouse gas. The avoidance of these emissions is an important reason why the bio-based pathway to succinic acid offers lower emissions. We considered two separation techniques in the production of succinic acid, EDI and LLE. Cradle-to-grave GHG emissions for biosuccinic acid are about 1.4 kg CO_2e/kg less when LLE is used.

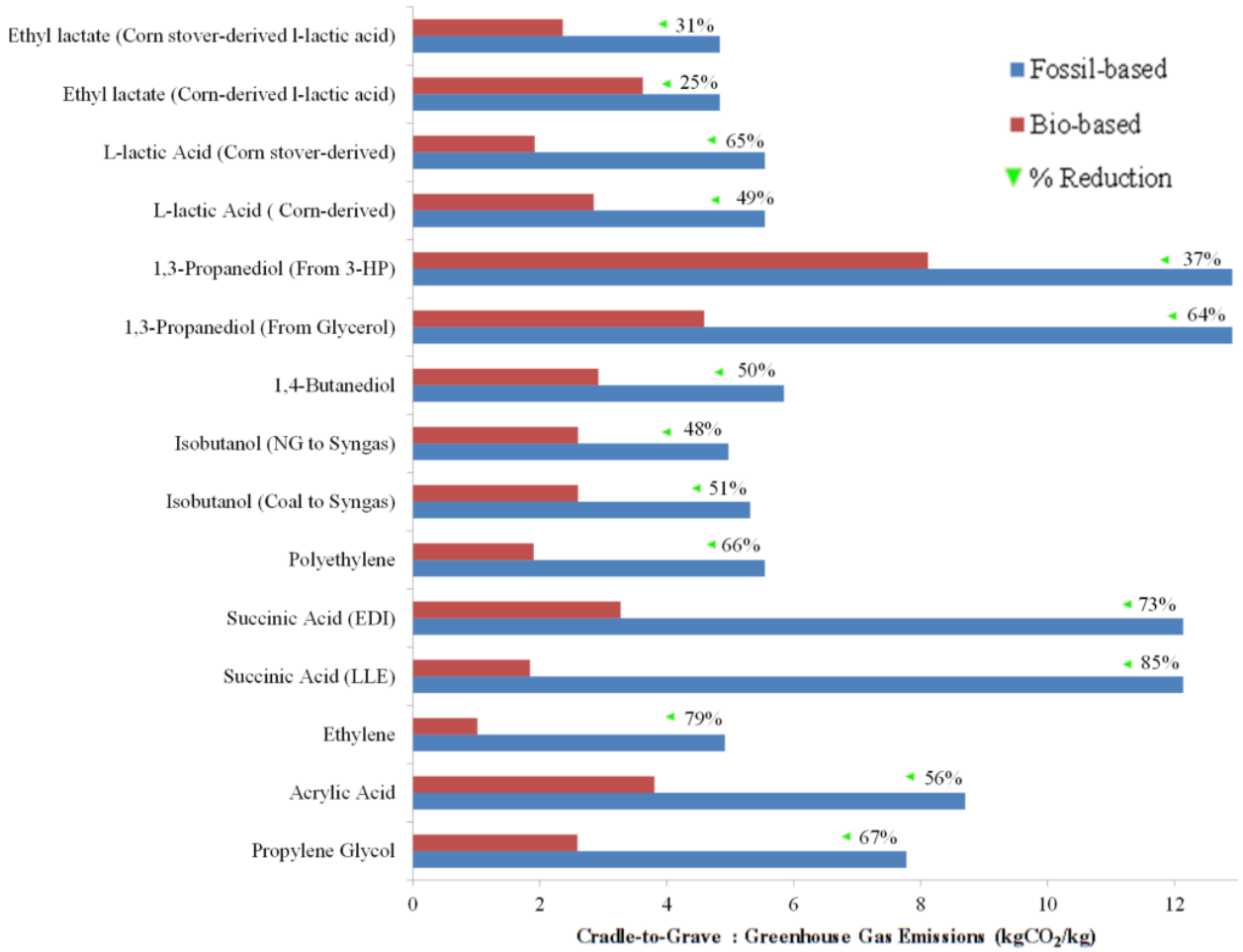

FIGURE 23 Summary of Cradle-to Grave GHG Emissions for Bioproducts

Figure 24 reports the cradle-to-gate fossil energy consumption of the compounds considered in this analysis. All of the bioproducts exhibit lower cradle-to-gate fossil energy consumption than their petroleum counterparts (24%–73%). Similar to the GHG trend (Figure 18), the highest savings was observed for biosuccinic acid. 1,3-PDO (from 3-HP) and isobutanol (natural gas to syngas) offered the least fossil energy consumption (FEC) savings of approximately 24% and 26%, respectively.

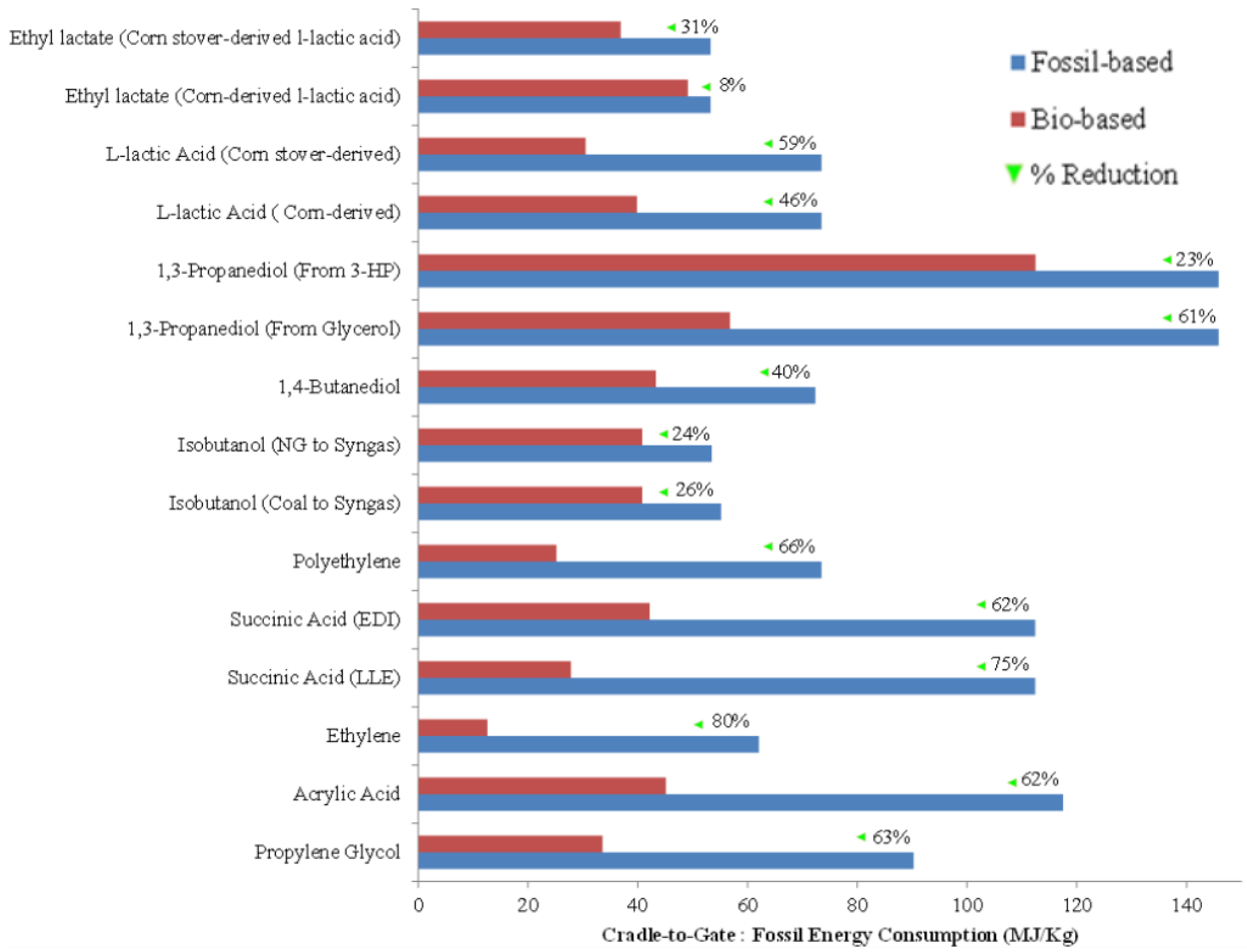

FIGURE 24 Summary of Cradle-to-Gate Fossil Fuel use for Bioproducts

Overall, this analysis illustrates that, for the most part, production of key compounds from biomass offers GHG and fossil energy savings compared to conventional, fossil-derived production of these same compounds. The new GREET module enables a robust and consistent analysis of bioproducts and can serve as a basis for companies and other interested parties to assess the relative energy and GHG performance of bio-based products.

This analysis used the best publicly available information to build the material and energy flow data that underpin the calculations. It is important to remember, however, that the current state of technology for bioproducts may be different than the public literature suggests. Additionally, data for conventional products based on Aspen simulations or engineering estimates provide approximations of energy and environmental burdens of producing these compounds, but it should be a priority to continue to seek out or build more refined analyses and data. The analysis could also be expanded to include process inputs of catalysts and microorganisms, which are currently excluded. Data for consumption of both of these inputs is highly proprietary and therefore has high associated uncertainty. Levels of microorganism consumption, for example, are difficult to extrapolate from bench-scale or patent data. It is

suspected, however, that the contribution of the production of these fermenting organisms may be minimal based on analyses of corn and cellulosic ethanol life-cycle impacts (Dunn et al. 2012a; MacLean and Spatari 2009). Life-cycle analysis of catalysts is an emerging area of research, but some biofuel life-cycle analyses suggest catalysts do not contribute significantly to biofuel life-cycle GHG emissions and energy consumption (Snowden Swan et al. 2013).

Future work could include refinement of existing Aspen simulations to reflect new information about these technologies. Additionally, sensitivity analysis to investigate the sensitivity of results to key assumptions such as yield and throughput could be undertaken. Furthermore, the processes were designed with an eye towards optimizing energy efficiency. They could be revisited to improve water efficiency and integrate waste water treatment. Additionally, an extension of the GREET bioproducts module to include additional compounds that Tables 2 and 3 include along with others that emerge as leading contenders for commercial-scale production could be beneficial.

7 REFERENCES

Acumedia. 2010. “Lactobacilli MRS Broth (7406).” http://www.neogen.com/Acumedia/pdf/ProdInfo/7406_PI.pdf.

Adams, Thomas A., and Warren D. Seider. 2008. “Semicontinuous Distillation for Ethyl Lactate Production.” *AIChE Journal* 54 (10): 2539–52. doi:10.1002/aic.11585.
ADM. 2015. “ADM-Fuels-and-Industrials-Catalog.” *ADM*. http://www.adm.com/en-US/products/Documents/ADM-Fuels-and-Industrials-Catalog.pdf.

Adom, Felix K., Jennifer B. Dunn, and Jeongwoo Han. 2014 (a). “Greet Pretreatment Module.” ANL/ESD-14/13. Argonne National Laboratory (ANL). http://www.osti.gov/scitech/biblio/1172036.

Adom, Felix, Jennifer B. Dunn, Jeongwoo Han, and Norm Sather. 2014 (b). “Life-Cycle Fossil Energy Consumption and Greenhouse Gas Emissions of Bioderived Chemicals and Their Conventional Counterparts.” *Environmental Science & Technology* 48 (24): 14624–31. doi:10.1021/es503766e.

Adom, Felix, and Jennifer B. Dunn, Argonne National Laboratory, unpublished information (2015).

ATCC. 2015. “Bacillus Coagulans Hammer (ATCC® 23498™).”
Atlas, Ronald M. 2010. *Handbook of Microbiological Media, Fourth Edition*. CRC Press.

Althaus, H., R. Hischier, M. Osses, A. Primas, S. Hellweg, N. Jungbluth, and M. Chudacoff. 2007. Life Cycle Inventories of Chemicals, Ecoinvent Report Number 8, Swiss Centre for Life Cycle Inventories, Dübendorf, CH.

Andreeßen, B., and A. Steinbüchel. 2010. “Biosynthesis and Biodegradation of 3-Hydroxypropionate-Containing Polyesters.” Applied and Environmental Microbiology, 75(15):4919–4925.

Avantium. 2013. “FDCA.” http://www.avantium.com/yxy/products-applications/fdca.html.

Baez, A., K. M. Cho, and J. C. Liao. 2011. “High-Flux Isobutanol Production Using Engineered Escherichia coli: A Bioreactor Study with in situ Product Removal.” Applied Microbiology and Biotechnology, 90(5):1681–1690.

Baker, J. 2013. “Cabot Takes the Plaudits for Aerogel.” ICIS Chemical Business, Oct. 21–27: pp. 1–15.
BASF. 2012. “BASF, Cargill and Novozymes Target Commercial Bio-based Acrylic Acid Process.” http://www.novozymes.com/en/news/news-archive/Pages/BASF-Cargill-and-Novozymes-target-commercial-biobased-acrylic-acid-process.aspx

Bastidon, A. I. 2012. “Biosuccinic Acid.” Nexant ChemSystems PERP Program. Report Abstract: PERP 2011S10. ChemSystems.com..

Bapat, Susmit S., Clint P. Aichele, and Karen A. High. 2014. “Development of a Sustainable Process for the Production of Polymer Grade Lactic Acid.” *Sustainable Chemical Processes* 2 (1): 3. doi:10.1186/2043-7129-2-3.

Barve, Prashant Purushottam, Bhaskar Dattatreya Kulkarni, Sanjay Narayan Nene, Ravindra William Shinde, Milind Yashwant Gupte, Chandrashekhar Narayan Joshi, Gandhali Arun Thite, Vilas Bhiku Chavan, and Tushar Ramchandra Deshpande. 2010. Process for preparing L- (+) - lactic acid. US7820859 B2, filed December 30, 2005, and issued October 26, 2010.

BD Bionutrients, Animal Free. 2015. “Bacto™ Yeast Extract BBL™ Yeast Extract Bacto™ Yeast Extract, Technical Difco™ Yeast Extract, UF.” *BD Bionutrients™ Technical Manual*, 25. Accessed June 19.

Bennett, Jacqueline S., Kaitlyn L. Charles, Matthew R. Miner, Caitlin F. Heuberger, Elijah J. Spina, Michael F. Bartels, and Taylor Foreman. 2009. “Ethyl Lactate as a Tunable Solvent for the Synthesis of Aryl Aldimines.” *Green Chemistry* 11 (2): 166–68. doi:10.1039/B817379F.

Bozell, Joseph J., and Gene R. Petersen. 2010. “Technology Development for the Production of Biobased Products from Biorefinery Carbohydrates—the US Department of Energy’s ‘Top 10’ Revisited.” *Green Chemistry* 12 (4): 539. doi:10.1039/b922014c.

Bell, B. M., et al. 2008. “Glycerin as a Renewable Feedstock for Epichlorohydrin Production. The GTE Process.” Clean Soil, Air, Water, 8:657–661.

BioAmber, Inc. 2012. “BioAmber Produces Biobased 1,4-Butanediol from Biosuccinic Acid.” BiomassMagazine.com. http://biomassmagazine.com/articles/7689/bioamber-produces-biobased-1-4-butanediol-from-biosuccinic-acid.

Bizzari, S. N. 2012. Chemical Economics Handbook Marketing Research Report Formaldehyde.

BlueFire Renewables. 2010. “BlueFire Renewables Holds the Key to a Better Future.” http://bfreinc.com/2010/06/c3-c3-homepage-post/.

Bournay, L., D. Casanave, B. Delfort, G. Hillion, and J. A. Chodorge. 2005. “New Heterogeneous Process for Biodiesel Production: A Way to Improve the Quality and the Value of the Crude Glycerin Produced by Biodiesel Plants.” Catalysis Today, 106:190–192.

Boussie, T. 2013. “Scale-Up and Commercialization of Bio-Based Adipic Acid and HMD.” Presented at the 4th Biobased Chemicals Commercialization & Partnering Conference, Sept. 16–17, San Francisco, CA.

Bozell, J.J., L. Moens, D. C. Elliott, Y. Wang, G. G. Neuenscwander, S. W. Fitzpatrick, R. J. Bilski, and J. L. Jarnefeld. 2000. "Production of Levulinic Acid and Use as a Platform Chemical for Derived Products." Resources, Conservation and Recycling, 28:227–239.

Bozell, J. J., and G. R. Petersen. 2010. "Technology Development for the Production of Biobased Products from Biorefinery Carbohydrates—the U.S. Department of Energy's 'Top 10' Revisited." Greenchem, 12(4):539–554.

Burnham, A., J. Han, C. E. Clark, M. Wang, J. B. Dunn, and I. Palou-Rivera. 2011. "Life-Cycle Greenhouse Gas Emissions of Shale Gas, Natural Gas, Coal, and Petroleum." Environmental Science and Technology, 11:619–627.

Burnham, A., J. Han, A. Elgowainy, and M. Wang. 2014. Argonne National Laboratory, unpublished information.

BusinessWire. 2012. "Incitor Incorporated Receives $1.5 Million Series A Investment." http://www.businesswire.com/news/home/20120611006638/en/Incitor-Incorporated-Receives-1.5-Million-Series-Investment#.UyifvO-L6Hc.

Cai, H., F. Grant, V. Divita, M. Wang, A. Elgowainy, and J. Han, Argonne National Laboratory, unpublished information (2014).

Chang, C., X. Ma, and P. Cen. 2006. "Kinetics of Levulinic Acid Formation from Glucose Decomposition at High Temperature." Chinese J. Chem. Eng., 14(5):708–712.

ChemSystems. 1998. "Polyaspartic Acid (96/97S4)." PERP Program. Prospectus. ChemSystems.com.

Chen, X., K. Tian, D. Niu, W. Shen, G. Algasan, S. Singh, and Z. Wang. 2014. "Efficient Bioconversion of Crude Glycerol from Biodiesel to Optically Pure D-lactate by Metabolically Engineered Escherichia coli." Green Chem., 16:342–350.

Chinn, H., and T. Kumamoto. 2011. Chemical Economics Handbook Product Review Propylene Glycols.

Chung, S. H., Y. M. Park, M. S. Kim, and K. Y. Lee. 2012. "The Effect of Textural Properties on the Hydrogenation of Succinic Acid Using Palladium Incorporated Mesoporous Supports." Catalysis Today, 185(1):205–210.

Chung, M.H., Y. K. Hong, H. W. Lee, and S. J. Park. 2013. "Aqueous Two Phase Extraction for the Recovery of 1, 3-Propanediol from its Aqueous Solutions." Advances in Materials Physics and Chemistry, 2:154

Cok, B., I. Tsiropoulos, A. L. Roes, and M. K. Patel. 2014. "Succinic Acid Production Derived from Carbohydrates: An Energy and Greenhouse Gas Assessment of a Platform Chemical toward a Bio-based Economy. Biofuels Bioprod. Biorefining, 8:16–29.

Colley, S. W., J. Tabatabaei, K. C. Waugh, and M. A. Wood. 2005. "The Detailed Kinetics and Mechanism of Ethyl Ethanoate Synthesis over a Cu/Cr2O3 Catalyst." *Journal of Catalysis* 236 (1): 21–33. doi:10.1016/j.jcat.2005.09.012.

Craciun, L., G. P. Benn, J. Dewing, G. W. Schriver, W. J. Peer, B. Siebenhaar, and U. Siegrist. 2009. U.S. Patent No. 7,538,247. U.S. Patent and Trademark Office, Washington, DC.

Curzons, A. D., D. C. Constable, and V. L. Cunningham. 1999. "Solvent Selection Guide: A Guide to the Integration of Environmental, Health and Safety Criteria into the Selection of Solvents." *Clean Products and Processes* 1 (2): 82–90. doi:10.1007/s100980050014.

Davis, M., et al. 2012. Renewable Diesel from Algal Lipids: An Integrated Baseline for Cost, Emissions, and Resource Potential from a Harmonized Model. Argonne National Laboratory Technical Report ANL/ESD/12-4.

Davis, R., D. Fishman, E. Frank, M. Wigmosta, A. Aden, A. Coleman, P. Pienkos, R. Skaggs, E. Venteris, and M. Wang. 2012. Renewable Diesel from Algal Lipids: An Integrated Baseline for Cost, Emissions and Resource from a Harmonized Model. Technical Report: ANL/ESD/12-4; NREL/TP-5100-55431; PNNL-21437. Argonne National Laboratory, Argonne, IL; National Renewable Energy Laboratory, Golden, CO; Pacific Northwest National Laboratory, Richland, WA.

Davis, R., et al. 2013. Process Design and Economics for the Conversion of Lignocellulosic Biomass to Hydrocarbons: Dilute-Acid and Enzymatic Deconstruction of Biomass to Sugars and Biological Conversion of Sugars to Hydrocarbons. Technical Report NREL/TP-5100-60223. http://www.nrel.gov/docs/fy14osti/60223.pdf.

Davis, S., and C. Funada. 2011. Chemical Economics Handbook Product Review Acetylene.

De Greyt, I. W. 2011. "Introduction on Glycerol as Co-product from Biodiesel Plants." Presented at Innovative Uses of Glycerol from Biodiesel Plants, Dec. 13, Brussels, Belgium.

De Guzman, D. 2013. "BioAmber Supplies Bio-succinic Acid in Europe." http://greenchemicalsblog.com/2013/06/12/bioamber-supplies-bio-succinic-acid-in-europe/.

Delgado, Patricia, María Teresa Sanz, Sagrario Beltrán, and Luis Alberto Núñez. 2010. "Ethyl Lactate Production via Esterification of Lactic Acid with Ethanol Combined with Pervaporation." *Chemical Engineering Journal* 165 (2): 693–700.
DOE and NETL (U.S. Department of Energy and National Energy Technology Laboratory). 2013. Analysis of Natural Gas-to-Liquid Transportation Fuels via Fischer-Tropsch. DOE/NETL-2013/1597.

DOE and NETL. 2007. Baseline Technical and Economic Assessment of a Commercial Scale Fischer-Tropsch Liquids Facility. DOE/NETL-2007/1260.

DOE EERE (U.S. Department of Energy, Energy Efficiency & Renewable Energy). 2012. "Pilot Integrated Cellulosic Biorefinery Operations to Fuel Ethanol." https://www1.eere.energy.gov/bioenergy/pdfs/ibr_arra_icm.pdf.

Ding, Z., J. Chiu, and W. Jin. 2013. U.S. Patent No. 8,394,999. U.S. Patent and Trademark Office, Washington, DC.

Dunn, Jennifer, Felix Adom, Jeongwoo Han, Norm Sather, and Seth Snyder, Argonne National Laboratory, unpublished information (2014).

Dunn, J. B., S. Mueller, H. Kwon, and M. Wang. 2013. "Land-use Change and Greenhouse Gas Emissions from Corn and Cellulosic Ethanol." Biotechnology for Biofuels, 6:51.

Dunn, J. B., S. Mueller, M. Wang, and J. Han. 2012a. "Energy Consumption and Greenhouse Gas Emissions from Enzyme and Yeast Manufacture for Corn and Cellulosic Ethanol Production." Biotechnology Letters, 34:2259–2263.

Dunn, Jennifer, Linda Gaines, Matthew Barnes, J Sullivan, and Michael Wang. 2012b. "Material and Energy Flows in the Materials Production, Assembly, and End-of-Life Stages of the Automotive Lithium-Ion Battery Life Cycle." Technical Report ANL/ESD/12-3 Rev. Argonne National Laboratory.

Dusselier, Michiel, Pieter Van Wouwe, Annelies Dewaele, Ekaterina Makshina, and Bert F. Sels. 2013. "Lactic Acid as a Platform Chemical in the Biobased Economy: The Role of Chemocatalysis." *Energy & Environmental Science* 6 (5): 1415. doi:10.1039/c3ee00069a.

Dutia, Pankaj. 2004. "Ethyl Acetate: A Techno-Commercial Profile." *CHEMICAL WEEKLY-BOMBAY-* 49: 179–86.

Dutia, P. 2008. "Phthalic Anhydride: A Techno-Commercial Profile Part 2: International Scenario." Chemical Weekly, Jan. 8.

Eerhart, A. J. J. E., A. P. C. Faaij, and M. K. Patel. 2012. "Replacing Fossil Based PET with Biobased PEF; Process Analysis, Energy and GHG Balance." Energy Environ. Sci., 5:6407–6422.

EC (European Commission). 2003. Integrated Pollution Prevention and Control (IPCC) Reference Document on Best Available Techniques in the Large Volume Organic Chemical Industry.

Endo, A., Y. Futagawa-Endo, and L.m.t. Dicks. 2011. "Influence of Carbohydrates on the Isolation of Lactic Acid Bacteria." *Journal of Applied Microbiology* 110 (4): 1085–92. doi:10.1111/j.1365-2672.2011.04966.x.

Evers D., D. Tolle. B.Vigon, S. Ricci, S. Freeman, K. Humphreys, C. Wend, and R. Landucci. 1997. "Streamlined Life-Cycle Assessment of 1,4 Butanediol Produced from Petroleum

Feedstocks versus Bio-derived Feedstocks." U.S. EPA, NRMRL, Systems Analysis Branch Cincinnati, Ohio.

Fan, D., D. Der-Jong, and H.-S. Wu. 2013. "Ethylene Formation by Catalytic Dehydration of Ethanol with Industrial Considerations." Materials, 6:101–115.

Franklin Associates. 2011. Cradle-to-Gate Life Cycle Inventory of Nine Plastic Resins and Four Polyurethane Precursors. Prepared for the Plastics Division of the American Chemistry Council.

Gannon, R. E., R. M. Manyik, C. M. Dietz, H. B. Sargent, and R. O. Thribolet. 2003. "Acetylene." In Kirk-Othmer Encyclopedia of Chemical Technology.

Gardett, P. 2012. "Cellulosic Ethanol Partnership Eyes Massive Potential Market." http://breakingenergy.com/2012/01/26/cellulosic-ethanol-partnership-eyes-massive-potential-market/.

GEVO. 2011. "Corporate Update." http://www.sec.gov/Archives/edgar/data/1392380/000119312511176342/dex991.htm.

Ghaffar, Tayyba, Muhammad Irshad, Zahid Anwar, Tahir Aqil, Zubia Zulifqar, Asma Tariq, Muhammad Kamran, Nudrat Ehsan, and Sajid Mehmood. 2014. "Recent Trends in Lactic Acid Biotechnology: A Brief Review on Production to Purification." *Journal of Radiation Research and Applied Sciences* 7 (2): 222–29. doi:10.1016/j.jrras.2014.03.002.

Ghanta, M., D. R, Fahey, D. H. Busch, and B. Subramaniam. 2013. "Comparative Economic and Environmental Assessments of H2O2-based and Tertiary Butyl Hydroperoxide-based Propylene Oxide Technologies." Sustainable Chemistry and Engineering, 1:268–277.

Girisuta, B., L. P. B. M. Janssen and H. J. Heeres. 2006. "Green Chemicals: A Kinetic Study on the Conversion of Glucose to Levulinic Acid." Chemical Engineering Research and Design, 84(5A):339–349.

Haas, T., B. Jaeger, R. Weber, S. F. Mitchell, and C. F. King. 2005. "New Diol Processes: 1,3-Propanediol and 1,4-Butanediol." Applied Catalysis A: General, 280:83–88.

Haro, P., P. Ollero, and F. Trippe. 2013. "Technoeconomic Assessment of Potential Processes for Bio-ethylene Production." Fuel Processing Technology, 114:35–48.

Harreus, Albrecht Ludwig, R. Backes, J.-O. Eichler, R. Feuerhake, C. Jäkel, U. Mahn, R. Pinkos, and R. Vogelsang. 2000. "2-Pyrrolidone." In *Ullmann's Encyclopedia of Industrial Chemistry*. Wiley-VCH Verlag GmbH & Co. KGaA. http://onlinelibrary.wiley.com/doi/10.1002/14356007.a22_457.pub2/abstract.

Heinzle, Elmar, Arno P. Biwer, and Charles L. Cooney. 2007. *Development of Sustainable Bioprocesses: Modeling and Assessment*. John Wiley & Sons.

Hermann, B. G., K. Blok, and M. K. P. Patel. 2007. "Producing Bio-based Bulk Chemicals Using Industrial Biotechnology Saves Energy and Combats Climate Change." Environmental Science and Technology, 41:7915–7921.

Holladay, J. E., J. F. White, J. J. Bozell, and D. Johnson. 2007. Top Value-Added Chemicals from Biomass Volume II—Results of Screening for Potential Candidates from Biorefinery Lignin. Pacific Northwest National Laboratory, Report No. PNNL-16983.

Hu, Jinlong, Zhenting Zhang, Yanxu Lin, Shumiao Zhao, Yuxia Mei, Yunxiang Liang, and Nan Peng. 2015. "High-Titer Lactic Acid Production from NaOH-Pretreated Corn Stover by Bacillus Coagulans LA204 Using Fed-Batch Simultaneous Saccharification and Fermentation under Non-Sterile Condition." *Bioresource Technology* 182 (April): 251–57. doi:10.1016/j.biortech.2015.02.008.

Huh, Y. S., Y. S. Jun, Y. K. Hong, H. Song, S. Y. Lee, and W. H. Hong. 2006. "Effective Purification of Succinic Acid from Fermentation Broth Produced by Mannheimia succiniciproducens." Process Biochemistry, 41(6):1461–1465.

Humbird, D., R. Davis, L. Tao, C. Kinchin, D. Hsu, A. Aden, P. Schoen, J. Lukas, B. Olthof, M. Worley, D. Sexton, and D. Dudgeon. 2011. Process Design and Economics for Biochemical Conversion of Lignocellulosic Biomass to Ethanol. National Renewable Energy Laboratory, Technical Report NREL/TP-5100-60223 [NREL/TP-5100-47764?].

IHS Chemical. 2011. "Polyisoprene Elastomers." http://www.ihs.com/products/chemical/planning/ceh/polyisoprene-elastomers.aspx.

INEOS Bio. 2013. "INEOS Bio Produces Cellulosic Ethanol at Commercial Scale." http://www.ineos.com/businesses/INEOS-Bio/News/INEOS-Bio-Produces-Cellulosic-Ethanol/?business=INEOS+Bio.

Ingledew, W. M. 2009. *The Alcohol Textbook: A Reference for the Beverage, Fuel and Industrial Alcohol Industries*. Nottingham University Press.

IPCC (Intergovernmental Panel on Climate Change). 2006. J. Harnisch, C. Jubb, A. Nakhutin, V. Cianci, R. Lanza, T. Martinsen, A. Mohammad, A. Santos, A. McCulloch, BT. Mader, J. Pérez-Ramírez, M. Neelis, M. Patel. IPCC Guidelines for National Greenhouse Gas Inventories. Prepared by the National Greenhouse Gas Inventories Programme, "Chapter 3: Chemical Industry Emission."

Jacques, Kathryn Ann, T. Pearse Lyons, and D. R. Kelsall. 2003. *The Alcohol Textbook: A Reference for the Beverage, Fuel and Industrial Alcohol Industries*. Nottingham University Press.

Javaid, Ahtesham, and Costin Sorin Bildea. 2014. "Integrated Production of γ-Butyrolactone through Coupling of Maleic Anhydride Hydrogenation and 1,4-Butanediol Dehydrogenation." *Periodica Polytechnica Chemical Engineering* 58 (2): 165–69. doi:10.3311/PPch.7303.

Javers, J. 2013. “ICM Generation 1.5 Cellulose to Ethanol.” http://www.fuelethanolworkshop.com/files/docs/2013/Javers_Jeremy.pdf.
Jong, Ed, Adrian Higson, Patrick Walsh, and Maria Wellisch. 2012. “Product Developments in the Bio-Based Chemicals Arena.” *Biofuels, Bioproducts and Biorefining* 6 (6): 606–24.

Karlen, D. L., and J. M. F. Johnson. 2014. “Crop Residue Considerations for Sustainable Bioenergy Feedstock Supplies.” BioEnergy Research, 7(2):465–67. doi:10.1007/s12155-014-9407-y.

Kosaric, Naim, Zdravko Duvnjak, Adalbert Farkas, Hermann Sahm, Stephanie Bringer-Meyer, Otto Goebel, and Dieter Mayer. 2000. “Ethanol.” In *Ullmann’s Encyclopedia of Industrial Chemistry*. Wiley-VCH Verlag GmbH & Co. KGaA. http://onlinelibrary.wiley.com/doi/10.1002/14356007.a09_587.pub2/abstract.

Lammens, T. M., et al. 2011. “Environmental Comparison of Biobased Chemicals from Glutamic Acid with Their Petrochemical Equivalents.” Environmental Science and Technology, 45:8521–8528.

Lane, J. 2012. “Virdia Ups the Ante in the Race for the New Sugars.” http://www.biofuelsdigest.com/bdigest/2012/03/06/virdia-ups-the-ante-in-the-race-for-the-new-sugars/.

Li, C., K. L. Lesnick, and H. Liu. 2013. “Microbial Conversion of Waste Glycerol from Biodiesel Production into Value-Added Products.” Energies, 6:4739–4768.

Lin, Y. 2013. Personal communication to Jennifer Dunn, Nov. 18.

Logsdon, John E. 2000. “Ethanol.” In *Kirk-Othmer Encyclopedia of Chemical Technology*. John Wiley & Sons, Inc. http://onlinelibrary.wiley.com/doi/10.1002/0471238961.0520080112150719.a01.pub2/abstract.

Ma, Z., L. Xu, X. Liao, H. Fang, B. Zhuge, and J. Zhuge. 2009 “Production of 1,3 propanediol from glycerol by engineered Escherichia coli using a novel coexpression vector.” Afr. J. Biotechnol., 8.

Maclean, H., and S. Spatari. 2009. “The Contribution of Enzymes and Process Chemicals to the Life Cycle of Ethanol.” Environmental Research Letters. doi://10.1088/1748-9326/4/1/014001.

Markets and Markets. 2013. “Global 1,3-Propanediol (1,3-PDO) Market Worth $560 Million by 2019.” http://www.marketsandmarkets.com/PressReleases/1-3-propanediol-pdo.asp.

Meng, Ying, Yanfen Xue, Bo Yu, Chenghua Gao, and Yanhe Ma. 2012. “Efficient Production of L-Lactic Acid with High Optical Purity by Alkaliphilic Bacillus Sp. WL-S20.” *Bioresource Technology* 116 (July): 334–39. doi:10.1016/j.biortech.2012.03.103.

Meng, X., T. W. Abraham, and P. Tsobanakis. 2006. “Process for Preparation of 1,3-Propanediol.” US7126034 B2, October 24.

Metabolix. 2013. “Metabolix Awarded Two U.S. Patents for Technology to Produce Biobased Polymers and Industrial Chemicals.” http://ir.metabolix.com/releasedetail.cfm?releaseid=667211.

Minh, D. P., et al. 2010. “Aqueous-Phase Hydrogenation of Biomass-Based Succinic Acid to 1,4-Butanediol Over Supported Bimetallic Catalysts.” Top Catal., 53:1270–1273.

Morgan, M. 2011. “Biomaterials: The Potential for Bio-Isoprene.” http://www.chemweek.com/chem_ideas/Guest-Author/Biomaterials-The-Potential-for-Bio-Isoprene_39990.html.

Moser, B. 2013. “Braskem Introducing LDPE Made from Sugarcane Ethanol.” http://www.plasticsnews.com/article/20130521/NEWS/130529974/braskem-introducing-ldpe-made-from-surgarcane-ethanol.

NanoChem Solutions. 2013. “About Polyaspartate.” http://nanochemsolutions.com/biopolymer/index.shtml.

Nelson, P.A, K.G Gallagher, I Bloom, and D.W Dees. 2011. “Modeling the Performance and Cost of Lithium-Ion Batteries for Electric-Drive Vehicles.” Technical Report ANL-11/32. Argonne, IL: Argonne National Laboratory.

Nextant. 2011. “ChemSystems, Process Evaluation/Research Planning: PERP 2011.”

Nexant. 2012. “Is Bio-Butanediol Here to Stay?” Prospectus. http://www.chemsystems.com/

Nexant. 2013. “From Diapers to Paints—Is Bio-Acrylic Acid on the Way?” Prospectus. http://thinking.nexant.com/sites/default/files/report/field_attachment_prospectus/201302/STMC11_Bio-Acrylic%20Acid_pros_r1.pdf.

Patel, Martin, Barbara Hermann, A.L Roes, and Leonard Overbeek. 2006. “The BREW Project: Medium and Long-Term Opportunities and Risks of the Biotechnological Production of Bulk Chemicals from Renewable Resources–the Potential of White Biotechnology.” Technical. The Netherlands: Technology and Society (STS)/Copernicus Institute, Utrecht.

Pavone, A. 2012. “Bio-based Adipic Acid.” Process Economics Program Report 284. http://www.ihs.com/products/chemical/technology/pep/bio-based-adipic-acid.aspx.

Pereira, Carla S. M., Viviana M. T. M. Silva, and Alírio E. Rodrigues. 2011. “Ethyl Lactate as a Solvent: Properties, Applications and Production Processes – a Review.” *Green Chemistry* 13 (10): 2658. doi:10.1039/c1gc15523g.

Posada, J. A., J. C. Higuita, and C. A. Cardona. 2011. “Optimization on the Use of Crude Glycerol from the Biodiesel Production to Obtain Poly-3-hydroxybutyrate.” Presented at the World Renewable Energy Congress 2011, May 8–13, Linköping, Sweden.

PRWeb. 2009. “Comet Biorefining Inc. Announces Cellulosic Sugar Technology.” Press Release. September 15. http://www.prweb.com/releases/2009/09/prweb2878784.htm.

Raj, S. M., C. Rathnasingh, J, Jo, and S. Park. 2008. “Production of 3-Hyroxypropionic Acid from Glycerol by a Novel Recombinant Escherichia coli Bl21 Strain.” Process Biochemistry, 43:1440–1446.

Reisch, MARC. 2008. “SOLVENT USERS LOOK TO REPLACE NMP.” *Chemical & Engineering News Archive* 86 (29): 32. doi:10.1021/cen-v086n029.p032.

Reisch, M. 2011. “The Sugar Makers.” Chemical & Engineering News, 89(47):20–21.

Righi, Serena, Andrea Morfino, Paola Galletti, Chiara Samorì, Alessandro Tugnoli, and Carlo Stramigioli. 2011. “Comparative Cradle-to-Gate Life Cycle Assessments of Cellulose Dissolution with 1-Butyl-3-Methylimidazolium Chloride and N-Methyl-Morpholine-N-Oxide.” *Green Chem.* 13 (2): 367–75. doi:10.1039/C0GC00647E.

Rivers, D. B. 2012. “Pathways to Clarified Sugars for Production of Fuels and Chemicals.” National Advanced Fuels Conference & Expo, Houston, TX.

Roweton, S., S. J. Huang, and G. Swift. 1997. “Poly(aspartic Acid): Synthesis, Biodegradation, and Current Applications.” Journal of Environmental Polymer Degradation, 5(3):175–179.

Saleh, A. 2011. “Myriant Succinic Acid BioRefinery (MySAB).” Myriant Lake Providence, Inc. BioMass Program IBR Platform Peer Review. Feb. 2.

Segetis. 2013. “Developing the Value Chain to Advance Levulinic Acid and Downstream Derivatives.” Presented at AGBiomass National Conference, Aug. 22, Ottawa, Canada.

Shuler, Michael L, and Kargi Fikret. 2002. *Bioprocess Engineering*. New York: Prentice Hall.
Sigma Aldrich. 2015. “Microbiology Products.” *Sigma-Aldrich*. Accessed June 19. http://www.sigmaaldrich.com/analytical-chromatography/microbiology/microbiology-products.html?TablePage=8657623.

Sims, B. 2012. “Sugar Rush.” http://biomassmagazine.com/articles/7751/sugar-rush.

Sims, B. 2011. “Canadian Co. Seeks to Penetrate Biobased Aspartic Acid Market.” http://biomassmagazine.com/articles/7500/canadian-co-seeks-to-penetrate-biobased-aspartic-acid-market.

Snowden-Swan, L. J., and J. L. Male. 2012. “Summary of Fast Pyrolysis and Upgrading GhG Analyses.” PNNL-22175. Pacific Northwest National Laboratory, Richland, WA (US). http://www.osti.gov/scitech/biblio/1072913.

SOLVAY S.A. 2010. “SOLVAY Goes Green Thanks to Epicerol: Using Glycerin as Renewable Feedstock Material for the Production of Epichlorohydrin.” Presented at KNCV Voorjaarsbijeenkomst NPT Sympsium Glycerol Valorisatie, April 15, Utrecht, Netherlands.

SRS Engineering Corporation. 2013. “What is Glycerin?” http://c1-preview.prosites.com/37030/wy/docs/Glycerin%20Purification.pdf.

Sweetwater Energy. 2013. “Sweetwater and Naturally Scientific Announce 15-Year, $250 Million Biochemical Project.” Press release. April 15. http://www.sweetwater.us/news/sweetwater-and-naturally-scientific-announce-15-year-250-million-biochemical-project.

Tao, L., E. C. Tan, R. McCormick, M. Zhang, A. Aden, X. He, and B. T. Zigler. 2014. “Techno- economic Analysis and Life- cycle Assessment of Cellulosic Isobutanol and Comparison with Cellulosic Ethanol and n- butanol.” Biofuels, Bioproducts and Biorefining, 8(1):30–48.

Urban, R. A., and B. R. Bakshi. 2009. “1,3-Propanediol from Fossils versus Biomass: A Life Cycle Evaluation of Emissions and Ecological Resources.” Industrial and Engineering Chemistry Research, 48:8068–8082.

US EPA (a). 2015. “Consolidated List of Chemicals Subject to the Emergency Planning and Community RightTo-Know Act (EPCRA), Comprehensive Environmental Response, Compensation and Liability Act (CERCLA) and Section 112(r) of the Clean Air Act.” United States Environmental Protection Agency. http://www2.epa.gov/sites/production/files/2015-03/documents/list_of_lists.pdf.

US EPA (b). 2015. “Alternatives / SNAP | US EPA.” *Ozone Layer Protection - Alternatives / SNAP*. Accessed July 30. http://www.epa.gov/ozone/snap/.

Vaidya, A. N., R. A. Pandey, S. Mudliar, M. Suresh Kumar, T. Chakrabarti, and S. Devotta. 2005. “Production and Recovery of Lactic Acid for Polylactide—An Overview.” *Critical Reviews in Environmental Science and Technology* 35 (5): 429–67. doi:10.1080/10643380590966181.

van Duuren, J. B. J. H., B. Brehmer, A. E. Mars, G. Eggink, V. A. P. Martins dos Santos, and J. P. M. Sanders, 2011. “A Limited LCA of Bio-Adipic Acid Using the Benzoic Acid Degradation Pathway from Different Feedstocks.” Biotechnology and Bioengineering, 108:1298–1306.

VCI. 2012. “Basic Chemicals Production 2030.” https://www.vci.de/Downloads/PDF/VCI%20analyis%20on%20the%20future%20of%20basic%20chemicals%20production%20in%20Germany.pdf.

Vertec Biosolvents. 2015. “Vertec Biosolvents.” *Vertec Biosolvents*. http://www.vertecbiosolvents.com/.

Waite, D. 2012. “Strategic Path to Bioproducts.” Presented at From Plants to Products: Seizing Maine’s Market Share in the Bio-Based Economy Seminar, April 11. http://mainebioplastics.org/wp-content/uploads/2012/04/Waite-4-11-12.pdf.

Walsh, Patrick, and Joachim Venus. 2013. Method for producing l (+) - lactic acid using bacillus strains. WO2013164423 A1, filed May 2, 2013, and issued November 7, 2013. http://www.google.com/patents/WO2013164423A1.

Wang, Z., J. Zhuge, H. Fang, and B. A. Prior, 2001. “Glycerol Production by Microbial Fermentation: A Review.” Biotechnology Advances, 19:201–223.

Wang, Q., I. V. Gürsel, M. Shang, and V. Hessel. 2013a. “Life Cycle Assessment for the Direct Synthesis of Adipic Acid in Microreactors and Benchmarking to the Commercial Process.” Chemical Engineering Journal, 234:300–311.

Wang, Y., X. Nie, and Z. Liu. 2013b. “Study on Preparation of Levulinic Acid from Biomass and its Prospects.” Journal of Forest Products and Industries, 2(3):5–7.

Wang, Z., J. B. Dunn, J. Han, and M. Wang. 2013c. Material and Energy Flows in the Production of Cellulosic Feedstocks for Biofuels in the GREETTM Model. Argonne National Laboratory, Technical Report ANL/ESD-13/9.

Wang, Zhichao, Jennifer Dunn, Jeongwoo Han, and Michael Wang. 2014. “Updates to Corn Ethanol Pathway and Development of an Integrated Corn and Corn Stover Ethanol Pathway in GREET Model.” Technical Report ANL/ESD-14/11. Argonne National Laboratory.

Weigert, W.M., and H. Haschke. 1976. “Acrylic Acid and Derivatives.” In Encyclopedia of Chemical Processing and Design. J. J. McKetta (ed.), Marcel Dekker, New York, NY.

Werpy, T., and G. Petersen. 2004. “Top Value Added Chemicals From Biomass: Volume I: Results of Screening for Potential Candidates from Sugars and Synthesis Gas.” http://www.nrel.gov/docs/fy04osti/35523.

Westervelt, R. 2013. “Ethylene Outlook Muted by Weak Demand, Supply Surge.” http://www.chemweek.com/sections/basic_chemicals_plastics/Ethylene-outlook-muted-by-weak-demand-supply-surge_50823.html.

Wooley, R., and V. Putsche. 1996. Development of an ASPEN PLUS Physical Property Database for Biofuels Components. National Renewable Energy Laboratory, Golden, CO. MP-425-20685, pp. 1–38.

Xiao, Y., G. Xiao, and A. Varma. 2013. “A Universal Procedure for Crude Glycerol Purification from Different Feedstocks in Biodiesel Production: Experimental and Simulation Study.” Ind. Eng. Chem. Res., 52:14291–14296.

Yang, F., M. A. Hanna, and R. Sun. 2012. “Value-added Uses for Crude Glycerol—A Byproduct of Biodiesel Production.” Biotechnology for Biofuels, 5:13–23.

Yang, Peng-Bo, Yuan Tian, Qian Wang, and Wei Cong. 2015. “Effect of Different Types of Calcium Carbonate on the Lactic Acid Fermentation Performance of Lactobacillus Lactis.” *Biochemical Engineering Journal* 98: 38–46.

Ye, Lidan, Xingding Zhou, Mohammad Sufian Bin Hudari, Zhi Li, and Jin Chuan Wu. 2013. “Highly Efficient Production of L-Lactic Acid from Xylose by Newly Isolated Bacillus Coagulans C106.” *Bioresource Technology* 132: 38–44.
Zeman, H., M. Url, and H. Hofbauer. 2011. Autothermal Reforming of Hydrocarbon Fuels. http://www.aidic.it/icheap10/webpapers/279Zeman.pdf.

Zhang, D., M.A. Hillmyer, and W.B. Tolman. 2004. “A New Synthetic Route to Poly[3-hydroxypropionic acid] (P[3-HP]): Ring-Opening Polymerization of 3-HP Macrocyclic Esters.” Macromolecules, 37:8198–8200.

Zhang, Li, Xin Li, Qiang Yong, Shang-Tian Yang, Jia Ouyang, and Shiyuan Yu. 2015. “Simultaneous Saccharification and Fermentation of Xylo-Oligosaccharides Manufacturing Waste Residue for L-Lactic Acid Production by Rhizopus Oryzae.” *Biochemical Engineering Journal* 94 (February): 92–99. doi:10.1016/j.bej.2014.11.020.

Zhang, M., and Y. Yu. 2013. “Dehydration of Ethanol to Ethylene.” Ind. Eng. Chem. Res., 52(28):9505–9514.

Zhang, Y., B. R. Bakshi, and E. S. Demessie. 2008. “Life Cycle Assessment of an Ionic Liquid versus Molecular Solvents and Their Applications.” Environmental Science and Technology, 42:1724–1730.

Zheng, P., J. J. Dong, Z. H. Sun, Y. Ni, and L. Fang. 2009. “Fermentative Production of Succinic Acid from Straw Hydrolysate by Actinobacillus succinogenes.” Bioresource Technology, 100(8):2425–2429.

Energy Systems Division
9700 South Cass Avenue, Bldg. 362
Argonne, IL 60439-4815

www.anl.gov

Argonne National Laboratory is a U.S. Department of Energy
laboratory managed by UChicago Argonne, LLC